Wiley
International Journal of Polymer Science
Volume 2024, Article ID 9405259, 27 pages
https://doi.org/10.1155/2024/9405259

WILEY

Research Article

Evaluation of the Mechanical Performance and Structural Characterization of Hybrid Green Composites Based on *Periploca laevigata* Aiton and Wool Natural Fibers

Lalmi Rahmani,[1] **Mohammed Taher Gherbi**,[1,2] **Aribi Chouaib**,[3] **H. S. S. Aljibori**,[4] **M. N. Mohammed**,[5] **Salah Al-Zubaidi**,[6] **Oday I. Abdullah**,[7,8,9] **and Mohammed Fouad Ferhat**[10]

[1]*UDERZA Laboratory, University of El Oued, El Oued 39000, Algeria*
[2]*Department of Mechanical Engineering, University of El Oued, El Oued 39000, Algeria*
[3]*Research Unit: Materials, Processes and Environment, Boumerdes University, Boumerdès, Algeria*
[4]*Al-Warith Center for Crowd Engineering and Management Research, University of Warith Al-Anbiyaa, Karbala, Iraq*
[5]*Mechanical Engineering Department, College of Engineering, Gulf University, Sanad 26489, Bahrain*
[6]*Department of Automated Manufacturing Engineering, Al-Khwarizmi College of Engineering, University of Baghdad, Baghdad 10071, Iraq*
[7]*Energy Engineering Department, College of Engineering, University of Baghdad, Baghdad, Iraq*
[8]*Department of Mechanics, Al-Farabi Kazakh National University, Almaty 050040, Kazakhstan*
[9]*College of Engineering, Gulf University, Sanad 26489, Bahrain*
[10]*Faculty of Technology, Department of Process Engineering, University of El Oued, Al Qued 39000, Algeria*

Correspondence should be addressed to Salah Al-Zubaidi; salah.salman@kecbu.uobaghdad.edu.iq

Received 16 January 2024; Revised 2 June 2024; Accepted 17 August 2024

Academic Editor: Ulrich Maschke

Copyright © 2024 Lalmi Rahmani et al. This is an open access article distributed under the Creative Commons Attribution License, which permits unrestricted use, distribution, and reproduction in any medium, provided the original work is properly cited.

The current research is focused on developing and evaluating new composite materials that are reinforced with natural fibers to enhance sustainability and create environmentally friendly composites. The use of both wool and *Periploca laevigata* Aiton fibers was chosen in the construction of the hybrid composite due to their similar organic composition, while also taking into account their different properties such as weight, density, and water absorption capabilities. This combination created a composite material that is not only lightweight but also has little water absorption. To further improve the quality of the wool, a treatment involving cold plasma has been carried out to enhance the bonding between individual fibers. Vacuum infusion technology is used during the manufacturing process to ensure the quality of the composite materials by eliminating trapped air, allowing for consistent purity in each repetition. The fibers used in this study include untreated wool fibers, NaOH-treated wool fibers, and cold plasma–treated wool fibers. Wool fibers were treated with a 5% sodium hydroxide solution for 30 min, resulting in fiber degradation. The concentration of the solution was gradually reduced until it reached a practical level of 0.1%. The hybrid composite incorporates wool that has undergone plasma treatments, which are crucial for removing organic contaminants from surfaces, strengthening the surface layer, and altering the chemical structure. The electric field applied had a strength of 9 kV and a frequency of 60 Hz. Atmospheric air was employed as the gas, with a flow rate of 800 L/min, and the fiber treatment lasted for 60 min. An analysis of natural fibers using Fourier transform infrared (FTIR) and X-ray diffraction (XRD) unveiled similarities in the organic structures and chemical bonds shared between *Periploca laevigata* Aiton fiber and wool fibers, despite their unique origins. While wool fibers are animal-derived, *Periploca laevigata* Aiton fibers stem from plants. By identifying these parallels, a hybrid composite material was formulated by combining plasma-treated wool fibers with *Periploca laevigata* fibers. This resulted in a significant improvement in the tensile, flexural, and compressive properties of the composite, establishing it as a promising avenue for enhancing mechanical performance. The PLAF-WLF hybrid composite exhibited a remarkable tensile strength of 26.02 MPa and Young's modulus of 2.35 GPa, surpassing all other composites. In comparison,

the PLAF composite demonstrated an impressive tensile strength of 20.1 MPa and Young's modulus of 2.34 GPa. The PLAF-WLF hybrid composite exhibited the highest flexural load-bearing capacity of 253.15 N and Young's modulus of 1.21 GPa. PLAF-WLF demonstrates a hybrid compressive strength of 59.56 MPa, while its Young's modulus is 0.5 GPa. The mechanical analysis findings revealed that the hybrid composite incorporating cold plasma–treated wool fibers and *Periploca laevigata* Aiton fibers displayed superior mechanical characteristics. Additionally, the composite made of *Periploca laevigata* Aiton fibers, recognized for its lightweight nature, smooth surface, and high quality, showed notable mechanical properties as well.

Keywords: cold plasma; composites; epoxy; fiber; hybrid composite; mechanical characteristics; *Periploca laevigata* Aiton; polymer; vacuum infusion; wool

1. Introduction

The utilization of composite materials is increasing, progressively substituting conventional materials. To stay abreast of the swift technological advancements in various industries, it is crucial to concentrate on creating inventive alternative material designs. Polymer composites are deemed superior alternative materials because of their reduced weight, enhanced strength, and cost efficiency. Fiber reinforcement is commonly employed in polymer matrices like polyester and epoxy to produce fiber-reinforced polymer (FRP) composite materials. Nowadays, there are numerous synthetic fibers available, such as E-glass fiber and aramid fiber, that enhance mechanical properties across the board. However, these composites may face challenges in terms of environmental impact due to issues related to degradability, renewability, and recyclability [1]. With the progress in technology, it is now feasible to utilize the ecofriendly characteristics of plant-based materials, all while taking into account environmental issues and sustainability factors. Consequently, natural fiber composites are presently attracting more interest [2].

Therefore, green composites are now a mandatory substitute for nondegradable material due to the increasing demand for natural fiber–based products, which minimizes the environmental impact. Due to the promotion of sustainability, bioreinforced composites have gained attention from various industries, including agricultural crops, aerospace, construction, packaging, fire retardancy, and housings for laptop computers [3]. Academics are interested in integrating environmental fiber into modern engineering activities due to reducing the number of synthetic fibers in polymer composites obtained from petroleum resources [4].

A composite material comprising a polymer matrix and incorporated fibers has garnered widespread interest worldwide. In light of the prevailing global environmental challenges, there is a rising inclination among people to explore the optimal use of natural fibers in diverse applications [5]. Natural fibers offer numerous advantages for use in composite materials such as high elastic modulus, flexural strength, flexibility, low density, renewability, biodegradability, and recyclability. These characteristics have significantly increased the appeal of natural fiber–reinforced composites. However, natural fibers also come with inherent disadvantages, such as poor compatibility with polymer materials. The hydrophilic nature of natural fibers results in weak adhesion and moisture absorption, leading to compatibility issues in biocomposites. Therefore, pretreatment of natural fibers is necessary to enhance the biocompatibility between the fibers and matrix through the activation of the fiber's hydroxyl groups [6].

Polymers are typically hydrophobic, while natural fibers are hydrophilic. Material scientists are currently developing numerous polymer composites using natural fibers that are easily accessible. In order to enhance the mechanical properties and environmental performance of these composites, natural fibers need to undergo chemical modifications with suitable additives or be coated with appropriate resins. Recent applications of chemical treatments include acetylation, alkali, acylation, silane, and benzoylation [7]. Among these, alkali treatment stands out as the most cost-effective and commonly used method. This treatment works by breaking down the hydrogen bonds in fiber bundles into smaller fibers, thereby reducing hydrophilic clusters in the matrix/fiber interaction [8]. Various methods are used to improve the adhesion between fiber morphology and the polymeric matrix. Sodium hydroxide (NaOH) and cold plasma techniques are commonly employed for this purpose. Cold plasma treatment, a physical method, is utilized to enhance the compatibility of natural fibers with the matrix. The fiber-matrix interface plays a crucial role in determining the quality of a fiber-reinforced composite. Acting as a binder, this interface facilitates the transfer of stress between the fibers, and it is enhanced through the use of a chemical agent such as NaOH. During the treatment process, water is taken in a specific volume along with 0.1% NaOH. The fibers are then soaked in this solution for a duration of 1 h. Subsequently, the fibers are meticulously washed with distilled water to eliminate any remaining alkali residues [9].

Plant, animal, and mineral fibers are categorized into broad classifications. Plant fibers consist of cellulose, hemicellulose, and lignin, whereas animal fibers contain various types of functional amino acids. Notably, cotton, jute, wool, and silk fibers are significant natural fibers that find extensive use in apparel clothing [10]. Wool plays a significant role in textile manufacturing as one of the key animal fibers. Like other hairs, animal horns, and fingernails, wool consists of a special protein called keratin, which sets it apart with its high sulphur content. With a chemical formula of NH2.CHR.COOH, wool is preferred over other fibers for its exceptional natural properties including feel, moisture absorption, strength, and its ability to hang. In contrast, wool stands out as the most contaminated natural fiber. A ton of raw wool typically comprises around 150 kg of lanolin, 40 kg of saint, 150 kg of dirt, 20 kg of vegetable matter, and merely 640 kg of wool fiber. Prior to its utilization in textile production, wool must undergo several treatment

procedures [11]. *Periploca laevigata* Aiton (PLA) subsp. angustifolia (Labill.) Markgraf, also known as *P. laevigata* Aiton or *P. angustifolia* Labill., is a plant species native to the Mediterranean and Saharan regions. It can be found growing naturally in the lower and middle basin areas, extending southwards into the northern and central Sahara. It is highly desired due to its conventional healing attributes and its significance in pastoral and erosion prevention, owing to its acclaimed medicinal properties. The *Periploca* species that have been extensively researched exhibit a range of biological activities, including antiproliferative, antitumor, and hypotensive effects [12].

Natural FRP composite is currently growing in industrial applications and scientific research due to their renewable nature, low cost, partially or completely recyclable, and biodegradability. Researchers have developed composite manufacturing techniques that use biodegradable natural fibers such as flax, cotton, hemp, jute, sisal, pineapple, banana, wood, date palm, and other fibers to manufacture products that have good mechanical properties and cost-effectiveness while minimizing environmental impact [13]. The reinforcement fibers are classified into two main groups: synthesized and natural fibers. Some plant fibers are good substitutes for synthesized fibers in different applications [14–16]. Animal fibers have low density and low cost. They are also readily available, with a constant supply, and they are safe to handle [17]. Animal fibers have diverse applications and are used in various sectors such as biomedical, construction, and automotive [18]. The producers of keratin fibers are largely dependent on the sheep wool fibers that play as raw materials for the textile industry. Some attempts were carried out to examine their thermal properties. For example, Zach et al. [19] examined the suitability of wool as thermal insulation in buildings and evaluated the wool at different temperatures. According to the findings, sheep wool insulation is comparable in performance with mineral or rock insulation. In some cases, it even performs better.

The materials are evaluated for their physical aspects as well as their mechanical properties to develop a better product and reach customer satisfaction [20]. Understanding natural fiber's physical and chemical properties, as well as mechanical characteristics, is required to increase composite material performance [21]. Depending on the nature and structural properties of the natural fiber, the use of natural fiber in the polymeric matrices allows us to adjust or improve some essential characteristic behaviors such as mechanical, thermal, acoustical, processing, and free volume [22]. The poor surface adhesion between the fiber and the polymer matrix is due to the hydrophobic nature of the fiber. Moisture penetration into composites can damage their mechanical characteristics in three different ways: the first mechanism involves the diffusion of water molecules into microgaps across polymer chains, the second mechanism involves the movement of filaments through gaps and defects in the fiber matrix contacts, and the third mechanism involves swelling effects, which cause microcracks to propagate in the matrix [23]. Several chemical treatments can be applied to the fiber surfaces to improve interfacial interaction and moisture absorption in natural fiber composites. Alkaline solution treatments improve the removal of partially amorphous elements such as hemicellulose, lignin, waxes, and oils soluble in alkaline solution and reduce the fiber diameter and degree of fiber clumping. The rough surface improves fiber/matrix adhesion [24]. There are some physical and chemical processes used in the treatment of fiber morphology to promote adhesion with the polymeric matrix. For instance, chemical treatment by NaOH and cold plasma methods. Cold plasma represents a form of physical treatment employed to enhance the compatibility of natural fiber with the matrix. Surface modification depends on the type and nature of the gas used [25]. Alkaline treatment represents the most commonly utilized method for treating plant fiber composites due to its low cost. This process effectively removes noncellulosic components from the fiber surface, resulting in a smooth and textured surface that enhances interfacial adhesion [17]. Alkaline treatment helps remove hydrogen bonds from the network structure of the fiber, which effectively reduces moisture absorption and reduces the diameter of the fiber, which raises the aspect ratio. Alkaline treatment enhances surface roughness, which increases mechanical cross-linking and exposes more cellulose on the surface of the fiber [18]. The NaOH procedure aims to enhance the contact area by reducing the presence of hydrophilic groups that result in an inadequate polymer matrix and weak fiber-matrix adhesion. The fibers undergo treatment with a NaOH chemical solution to enhance the interfacial adhesion between the fibers and matrix, thereby achieving tensile strength through a well-established interface along the fiber surface [4].

There are a number of studies that promote the use of sheep's wool as a toughening agent in an epoxy matrix. In order to assess the mechanical properties of composites, various forms of sheep wool were tested as toughening agents in an epoxy matrix [26, 27]. Therefore, wool fibers can be used as good strengtheners for polymeric matrix not only for the improvement of the thermal properties but also it is extended to mechanical properties as will be seen in the current study.

The exploration of a new hybrid composite, which combines cold plasma–treated wool fiber (WLF) and PLA, represents a cutting-edge project in materials science. A thorough investigation of the existing literature reveals no documented cases where this specific compound has been synthesized. By subjecting wool fibers to cold plasma treatment and incorporating *P. laevigata* Aiton fibers (PLAF), this innovative approach aims to capitalize on the unique properties of both fibers to improve composite performance. The production of such a hybrid composite highlights the pioneering nature of this research, opening up possibilities for new applications and developments in the field of composite materials. As the scientific community aims to push the frontiers of materials science forward, the synthesis of animal-based wool fibers treated in a cold plasma environment with plant-based PLA emerges as a promising and unprecedented method for developing advanced hybrid composites.

The main contribution of the current study is to manufacture and investigate the performance of a new hybrid

green composite processed from the reinforcement of epoxy resin with untreated PLAF and WLF. For comparison purposes, another three composites were fabricated with epoxy resin reinforced with untreated WLF, chemically treated NWLF by NaOH, and untreated PLA. The structure of four fibers was characterized by Fourier transform infrared (FTIR), X-ray diffraction (XRD), and scanning electron microscopy (SEM). Four composite materials were fabricated from different volume fractions of natural fibers and epoxy resins by the vacuum infusion method. All composites were subjected to three mechanical tests, namely, tensile, flexural, and compression tests, to show the effectiveness of hybridizing the PLAF-WLF composite with PLAF fiber.

2. Materials and Procedures

This section presents a description of the two natural fibers being used in this study, namely, PLA and wool fibers. Also, it illustrates how these two fibers are prepared and treated to examine their structures by using FTIR and XRD. It also describes how the composite materials were produced. Further, it shows how the produced composite materials are subjected to tensile, compression, and flexure tests.

Figure 1 depicts the adopted methodology in this study which shows the steps mentioned above. It reveals that the applied methodology consists of several steps to reach the proposed objectives of the current study. These steps are described in the following subsections.

2.1. Preparation of the Natural Fibers

2.1.1. PLAF. PLA is actually a heat-loving, perennial, deciduous shrub that is widespread in different regions. It is native to the Mediterranean region and can be found in countries such as Spain, Algeria, Libya, Tunisia, Karpathos, Egypt, Crete, Malta, and Sicily [28]. PLA has drooping leaves and an entire, narrowly lanceolate branch. The flowers are distributed in short auxiliary cymes with reddish-brown lobes bordered in greenish-yellow and alternated with incurved purplish filaments. The fruit is dry and made up of two smooth and fissured follicles that contain anemocorous seeds [29]. These fibers are short and very lightweight; they fly in the air after the lobes become dry, and they crack naturally, as shown in Figures 2(a), 2(b), and 2(c). It has not undergone any processing due to its delicate structure and natural characteristics. The PLA lobes were manually extracted by opening the lobes and separating the seeds from the fiber. The fibers were washed extensively with distilled water at 25°C. This temperature maintains the structural characteristics of the fiber. The fiber was filtered and then subjected to a 24-h drying process at room temperature.

Archimedes' principle was employed to determine the density of PLAF. The fibers of 4.5 g mass were impressed in a 100 mL water container to calculate the volume difference. The fiber's mass (4.5 g) is divided by its volume (0.01 L) to get the fiber density of 0.45 g/cm^3.

2.2. Preparation and Treatment of Wool Fiber. Sheep wool, alpaca hair, goat hair, horse hair, and other hairy mammal fiber are examples of animal fiber [30]. Wool has long been used in the clothing and textile industries, and it will continue to assume a significant role in a number of new and future uses [31]. Shearing, washing, drying, grading, sorting, carding, spinning, weaving, and finishing are all important processes in the process of turning wool from sheep into fabrics [30]. Wool samples are taken from sheep in the Ghardaia region (Algeria), and the wool was sheared from sheep in the spring, resulting in greasy raw wool that contained a lot of dirt, sand, oil, and dry sweat. A part of this wool was manually cleaned of dirt and dust; another part was treated with a NaOH solution with a concentration of 0.1%, and the last part was cleaned with cold plasma. The next two sections (2.2.1 and 2.2.1) describe how the WF has been treated by the second and third methods (i.e., chemical and cold plasma methods).

After cleaning the wool with the three previously mentioned methods, it is combed as it is passed through a series of thin metal teeth that work to loosen wrinkles and tangles in the fiber, and then it is arranged in the form of a flat strip called a weave, which later turns into thin threads. After the fibers are carded, the threads are stretched and twisted to make them thinner, just as the fibers are pulled to become very thin and ready for spinning. Figure 3 shows the manufacturing process depicted in the study.

2.2.1. Chemical Treatment Method. Natural fiber is hydrophilic in nature and has seen significant obstacles in polymeric composites due to the presence of its hydroxyl groups like lignin, cellulose, and waxes [32]. Because of their negative sensitivity to water, it is difficult to combine natural fiber with a hydrophobic matrix [33]. Therefore, the natural fibers must be treated before processing any green composite materials. The chemical treatment is generally applied to the natural fiber to remove impurities and other particles from the surface of the fiber, tightening the surface of the fiber and matrix to enhance the interfacial bonding between them [34, 35]. Alkaline treatment helps remove hydrogen bonds from the network structure of the fiber, which effectively reduces moisture absorption and reduces the diameter of the fiber, which raises the aspect ratio. Alkaline treatment enhances surface roughness, which increases mechanical cross-linking and exposes more cellulose on the surface of the fiber [36]. NaOH is one of the most important alkaline chemical treatments in this field [37]. Therefore, the NaOH treatment was nominated to process the fibers. We immersed the wool in a 5% solution of NaOH for 30 min, and the fiber started to degrade. Treatment of wool fiber with NaOH at different concentrations, specifically 5% and 3%, results in varying degrees of fiber structure breakdown. The concentration of the solution was gradually reduced until it reached a practical concentration of 0.1%, with every treatment taking 1 h. At this point, there is a rough surface with uniform roughness. The treated wool fibers were washed with distilled water and dried at ambient temperature (25°C) for 3 days. As a result, 0.1% NaOH was used during the fiber chemical treatment process in this experiment.

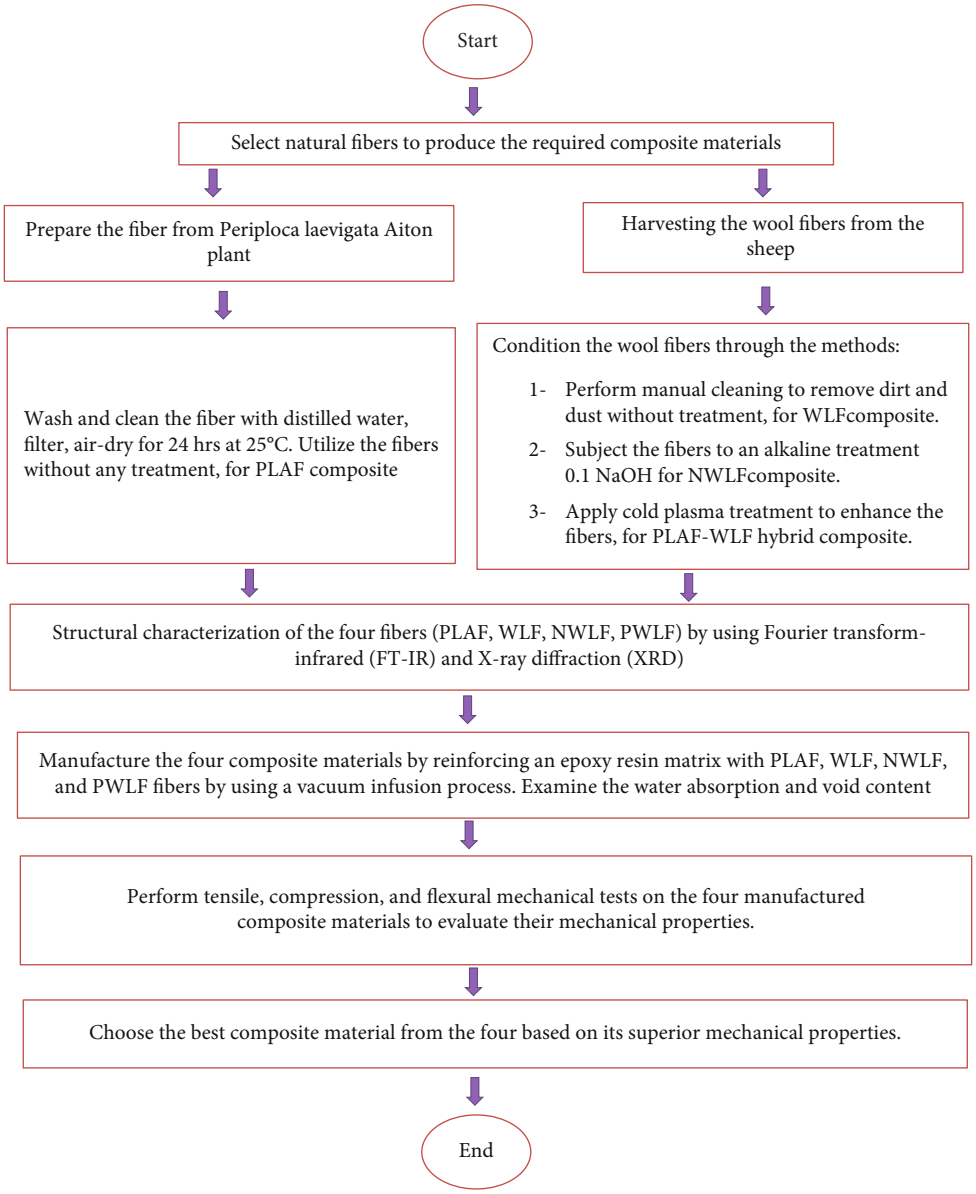


Figure 1: Applied methodology.

2.2.2. Cold Plasma Treatment Method. Plasma surface treatment is very important in the industrial field due to its efficiency and environmental friendliness [38]. The cold plasma treatment can be used to modify the surface of short glass, carbon, cellulose, polyimide, aramid, and other fibers. The surface of cellulose fiber was altered by air plasma treatment, which was employed to augment the adhesion between the thermoplastic starch matrix and the fiber. SEM analyses of the fractured surfaces demonstrate a considerable increase in adhesion between treated cellulose fiber and the thermoplastic starch matrix [39]. The applied electric field was generated using a gliding ARC discharge with a power source set at 9 kV at a frequency of 60 Hz. The atmospheric air was used as a gas, with a flow rate of 800 L/min. As shown in Figures 4 and 5, the plasma jet discharge extended approximately 5 cm, giving a direct measurement of the cold plasma's effect on natural fiber. The gliding arc discharge reactor consists of two diverging stainless steel electrodes with a thickness of 1 mm, located at the bottom of the feed gas nozzle. The fibers were put in a container 10 cm in diameter and 1 cm thick. The wool was treated with cold plasma inside a container containing distilled water. For a set period of time, the fiber was moved randomly inside the container under the effect of the plasma jet at ambient air temperature. During processing, the fiber was maintained 5 cm away from the flow of liquid plasma. Jet plasma treatment was applied to the fiber for a period of 60 min. Plasma-treated wool fiber was left in ionized water for 4 h. The wool fiber was washed with distilled water and left to dry at room temperature for 3 days before utilization, and the drying procedure was accomplished by subjecting it to an oven at a temperature of 60°C for a duration of 24 h.



(a) (b) (c)

Figure 2: *Periploca laevigata* plant and its fibers: (a) the *Periploca laevigata* Aiton plant, (b) lobes with fibers, and (c) extracted fibers.

2.3. Epoxy and Hardener. The resin matrix that is intended to be strengthened in this study by the natural fibers is Duraclear Epoxy. It is provided by AGEL Chemicals Company, and its properties and specifications are tabulated as Table 1 shows.

2.4. Structural Characterization of WF and PLA Natural Fibers

2.4.1. Analysis via FTIR. Researchers have experimented with a variety of chemical treatments to enhance the cellulose content, mechanical characteristics, surface roughness, and so on, and this method can be used to determine the chemical changes occurring in the functional groups. Analysis using the FTIR [41]. The samples were examined using FTIR (Shimadzu, IR Affinity-1, FTIR, Resolution 8). To study changes in chemical composition, 0.02 g of each sample was grinded and mixed with 0.198 g of KBr powder before being grinded on a KBr disk and compressed at a pressure of 70 kN for 2 min. FTIR uses a wavenumber range of 400–4000 cm^{-1}, and 20 scans were performed in each case.

2.4.2. Analysis Using XRD. X-ray crystallography is the most extensively utilized method for identifying the molecular and crystal structures of any crystalline substance, whether natural or synthetic [42]. The recording pattern is based on measuring diffraction line intensities by transmitting source and detector steps. We were able to record the diffraction pattern on the investigated material using the XRD instrument. XRD spectroscopy with wavelength $\lambda_{CuK} = 1.54^{\circ}A$ at 2θ scan angles ranging from 10° to 90°, whereas this approach allows for the determination of diffraction lines based on Bragg's law.

2.4.3. SEM. The SEM test would provide a complete view of the structural characterization of all natural fibers being used in the current study. All those fibers were subjected to SEM

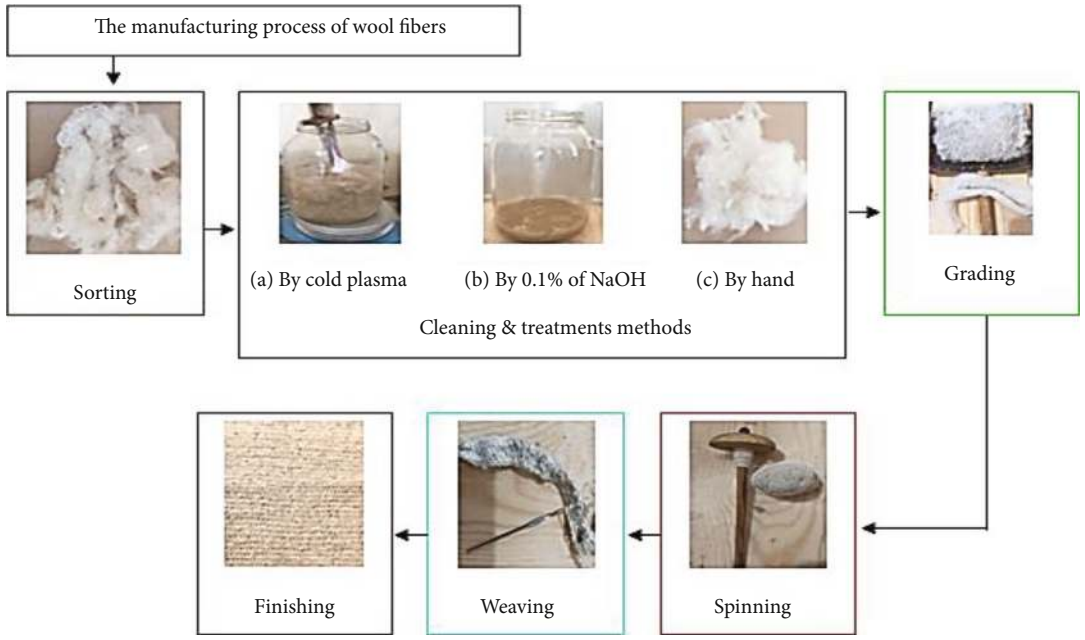


Figure 3: Preparation of the wool fiber: (a) cold plasma treatment, (b) treatment by 0.1% NaOH, and (c) manual cleaning.

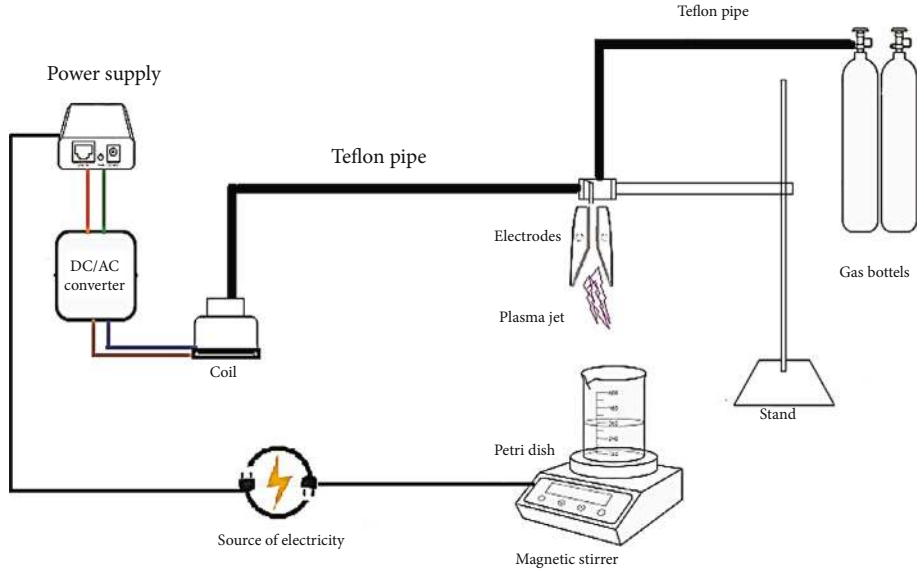


Figure 4: Cold plasma treatment process.

examination. It is a helpful tool in scanning and illustrating the surface features of all fibers.

The SEM (Leo Supra 55, Zeiss Inc., Oberkochen, Germany) was operated with specific settings for effective analysis. The voltage was set at 10 kV, the beam current at 5 μA, and the spot size at 10 nm. Additionally, the acceleration angle was adjusted to optimize the investigation of the morphology of the four composites. These meticulously chosen parameters aimed to ensure precise and detailed imaging during the SEM analysis.

2.5. Fabrication of Composite Materials. The vacuum infusion molding process was used in this study to manufacture composite material. This process can solve challenges with manual lay-up and spray-up methods. One of the modern composite manufacturing processes that could potentially replace the traditional method is the vacuum infusion molding process. The idea behind vacuum infusion is to create a vacuum and draw air into the mold through negative pressure while sucking the resin into the mold, thereby impregnating the reinforcement in the resin. The vacuum infusion molding process eliminates the risk of trapped air in the composite, and this process enables the composite to be manufactured in repetition with the same purity because it is dependent on the design of the equipment rather than the operator's competence [43].



Figure 5: Wool fiber under cold plasma jet.

Table 1: Properties and specifications of Duraclear Epoxy [40].

Item	Specifications
Density (specific density at 25°C)	1.12 epoxy, 0.97 hardener
Mix ratio (volume)	2:1
Mix ratio (weight)	100:43
Viscosity (A/B/mixed at 25°C)	1850/35/280
Mixed density-specific density at 25°C	1.07
Pot life at 25°C	90 min
Tack free time at 35°C	24 h
Color	White
pH	7–9
Recommended full cure	7 days at 25°C
Gel time @ 22°C in a 150-g mass	5.5 h
Maximum casting depth	1.27–2.54 cm

After the resin layer and matrix have been produced, excess resin will be extracted from the mold through suction. This method ensures homogeneous thickness distribution along the part. The material produced by the vacuum infusion technique has a greater fiber-to-resin ratio than the material produced by the hand lay-up method, resulting in a stronger and lighter composite material [44]. The mold has a dimension of 300 mm × 250 mm × 4 mm. Initially, fibers were weighed using a sensitive balance, and the amount of epoxy and hardener needed was calculated. The fibers, regardless of the type or treatment conditions, were dried in an oven at 60°C to prevent voids, moisture, and poor fiber-matrix adhesion. The mold surface was carefully cleaned, and a mold-releasing agent was coated all over the mold surface for easy removal and an excellent product surface finish. The fiber was placed in the mold once it had been prepared; after that, the mold was covered with another layer of mold. In Figure 6, we present the experimental setup, offering a clear depiction of the apparatus used for our study. The hose used for the inlet is attached to the resin tank, while the outlet hose is connected to the resin trap. After connecting and completing the circuit vacuum pump installation, it began to operate, and the resin flowed through the input section and entered the mold due to the pressure differences until it reached the output section. The vacuum pressure used to suction epoxy resin is 30 mHg. In Figures 7(a), 7(b), 7(c), 7(d), and 7(e), we outline the sequential steps involved in the manufacturing of the composites. The specimens depicted in Figures 8(a), 8(b), 8(c), and 8(d) were carefully positioned within a controlled environment. Previous findings in the literature suggest that the increase in wool fiber content has minimal influence on tensile stress or elastic modulus [45]. Various studies have employed volume fractions ranging from 30/70, 40/60, to 50/50. Notably, a volume fraction of 30/70 is considered the minimum, as any reduction below this ratio results in a decline in mechanical properties. Similarly, a volume fraction of 50/50 is considered the maximum, but the composition with a ratio of 50-50 exhibits higher moisture absorption compared to the composition with a ratio of 60-40, while the 60-40 composition demonstrates greater chemical absorption than the 50-50 composition [46]. When the fiber content surpasses 50%, the mechanical properties also deteriorate. To create a lightweight composite with favorable mechanical properties, our research highlights the significance of reducing the wool percentage and incorporating plant fibers. This combination enhances properties such as low water absorption, low density, and lightweight. Therefore, we selected a fiber percentage of 30% and maintained the same proportion when introducing plant fibers. As a result, we decreased the wool percentage in the composite. Table 2 presents the weight percentage compositions of the composite specimens, offering a comprehensive overview of their material compositions.

2.6. Mechanical Tests of the Composite Materials. After the fabrication of the four composite materials, all specimens were subjected to three mechanical tests, namely, tensile, compression, and flexural tests, to evaluate their response to different types of loading. The tensile and compression tests were conducted using the Zwick/Roell Z10 machine, which was controlled by test pert software Version 12.0 and equipped with a precision 10 kN force sensor. Conversely, for flexural examinations, it was utilized the Zwick Z 2.5 machine, which featured a 2 kN sensor. Figure 9 shows the universal Zwick/Roell Z10 tensile and compression and Zwick Z 2.5 Flexural tester. In order to compare the mechanical performance of each composite and achieve optimal results, we conducted assessments on five specimens for each structure. These assessments were carried out under consistent conditions, incorporating conditions such as ambient temperature and a testing speed of 5 mm/min. The tests provided valuable insights into the specimen's behavior, encompassing measurements such as elongation, nominal strain, Young's modulus, and tensile strength. Figure 10 outlines the dimensions of the tensile, compressive, and flexural specimens, as illustrated in Figure 11. The three tests were conducted according to ASTM D3039, ASTM D790, and D3410, respectively.

3. Water Absorption

3.1. PLAFs. The behavior of water absorption is commonly investigated in accordance with ASTM D 570. The

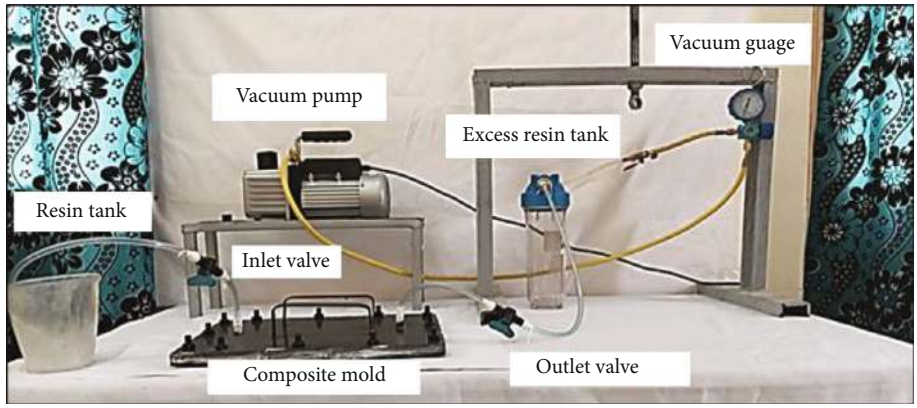


Figure 6: Vacuum infusion molding process.

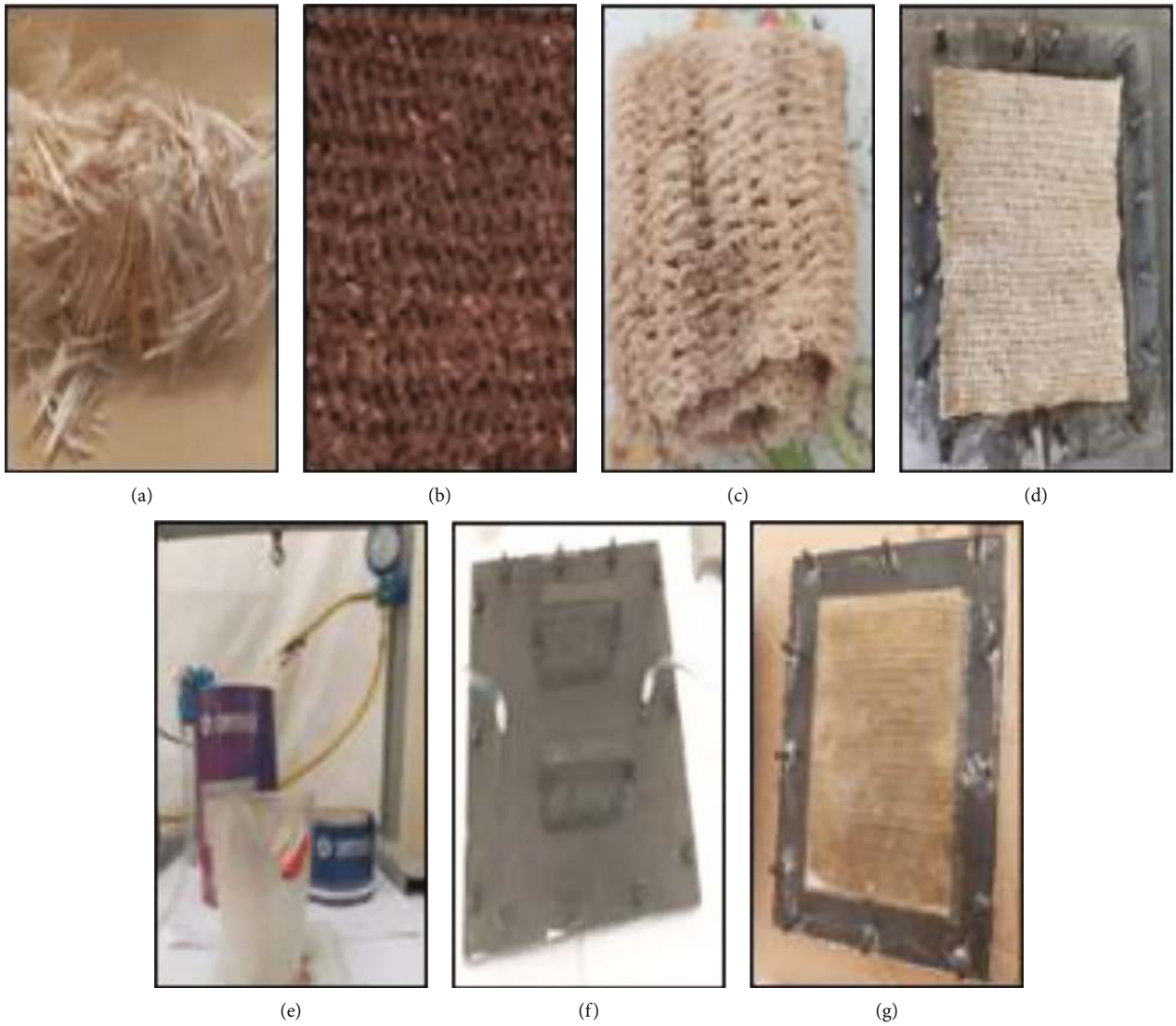


Figure 7: Manufacturing of composites by vacuum infusion molding: (a) *Periploca laevigata* Aiton fiber, (b) WLF, (c) NWLF, (d) PLAF-WLF, (e) epoxy and hardener, (f) closed mold, and (g) composite after curing time.



(a) (b) (c) (d)

Figure 8: Final composites specimens: (a) NWLF, (b) WLF, (c) PLAF-WLF, and (d) PLAF.

Table 2: Compositions of the composite specimens in weight percentage.

Type of fiber	Type of treatment	Fiber weight fraction (wt.%)	Epoxy resin weight fraction (wt.%)
WLF	Untreated	30	70
NWLF	NaOH-treated	30	70
PLAF	Untreated	15	85
PLAF-WLF	Untreated (PLAF), cold plasma–treated (WLF)	10/20	70

percentage increase in water absorption is calculated using a specific Equation (1) [47].

$$\text{Water absorption\%} = \frac{W2 - W1}{W2} \times 100 \quad (1)$$

where W_1 is the weight before soaking in water (gram) and W_2 is the weight after soaking in water (gram).

To begin the process, the samples were meticulously cleaned and then placed in individual containers filled with distilled water. They were left in the water for a duration of 10 min at room temperature. Each sample had a weight indicated in Table 3. Once the immersion period was complete, the samples were carefully removed from the containers. To facilitate the absorption of surface moisture, the fiber samples were positioned between a pair of filter papers and a pair of circular disks. The pressure exerted by the circular disk allowed the filter paper to absorb the moisture. Finally, the weights of the samples were measured using a precise digital balance machine in order to determine the percentage of water absorption [48].

As shown in Table 3, the water absorption of PLA ranges from 11.09% to 7.22%. This finding highlights another significant advantage of PLAFs, in addition to their lightweight nature.

Compared to various other natural fibers, such as cotton fibers (which can absorb water between 32.5% and 50.5%), banana fibers (which can absorb water between 495% and 448.5%), and raw areca fibers (which can absorb water between 698% and 851%), PLAFs exhibit a significantly lower rate of water absorption [28].

3.2. Wool Fibers. Wool, being a protein polymer, possesses various functional groups and an amorphous region, enabling it to readily absorb water molecules. It can retain water from 13% to 18% of its dry weight at 65% relative humidity, and this percentage can increase up to 40% at 100% relative humidity [49].

3.3. Void Content. Physical attributes play a crucial role alongside mechanical properties in assessing the suitability of a composite material for specific applications. Among these attributes, density stands out as a key factor. The theoretical density (Td) of composite samples measuring 25 mm × 25 mm × 4 mm, relative to their weight fraction, is calculated using Equation (2) as per ASTM D2734-94 [50].

$$Td = \frac{100}{R/D + r/d} \quad (2)$$

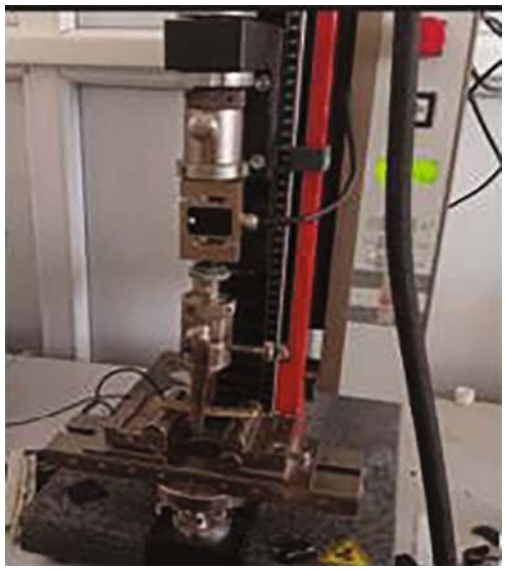
The actual density (Md) of the composite material is determined by dividing the weight by the volume. The composite void fraction (V) can be calculated using Equation (3) as per the ASTM D2734-94 standard. In this equation, Td represents the theoretical density in grams per cubic centimeter, R represents the weight fraction of resin, D represents the density of resin in grams per cubic centimeter, r



(a) Tensile machine



(b) Compression machine



(c) Flexural machine

Figure 9: Test machines: (a, b) universal Zwick/Roell Z10 tensile and compression tester and (c) Zwick Z 2.5 Flexural tester.

represents the weight fraction of fiber, and d represents the density of fiber in grams per cubic centimeter [50].

$$V = \frac{100(Td - Md)}{Td} \tag{3}$$

The void fraction, denoted as V, is expressed in volume percentage. Td represents the theoretical density of composites in grams per cubic centimeter, while Md represents the actual (measured) density of composites, also in grams per cubic centimeter.

The table provided in Table 4 displays the void fraction in relation to the measured and theoretical densities of the composites.

The decrease in void fraction observed when blending PLAFs in the hybrid composite can be attributed to multiple factors. The addition of these fibers reduces the presence of voids or empty spaces between the fibers. This is due to enhanced interaction between the fibers and the matrix, as well as a decrease in shrinkage and buckling during the curing process. As a result, the total area available for voids is reduced, leading to a denser arrangement of materials in the composite and a lower void ratio. This improved filling efficiency ultimately contributes to the reduction in void fraction.

4. Results and Discussions

As aforementioned above, the structural characteristics of untreated PLA and treated and untreated WLF fibers were analyzed by using FTIR, XRD, and SEM. On the other hand, the composite materials, which were processed from those

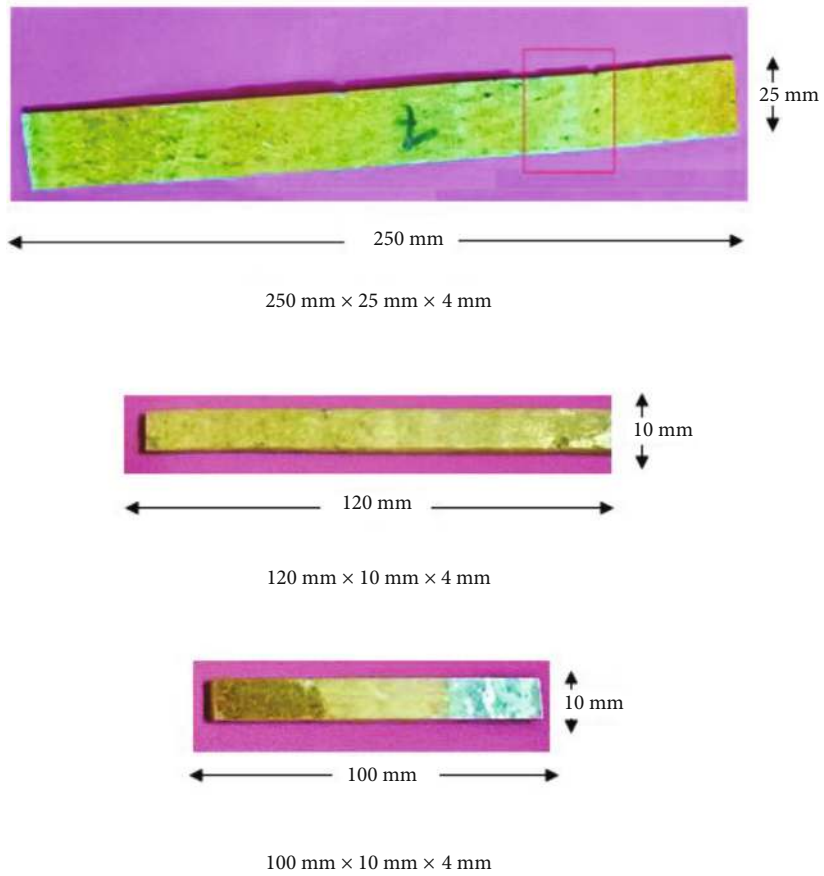


Figure 10: Specimen dimensions for tensile, flexural, and compression tests.

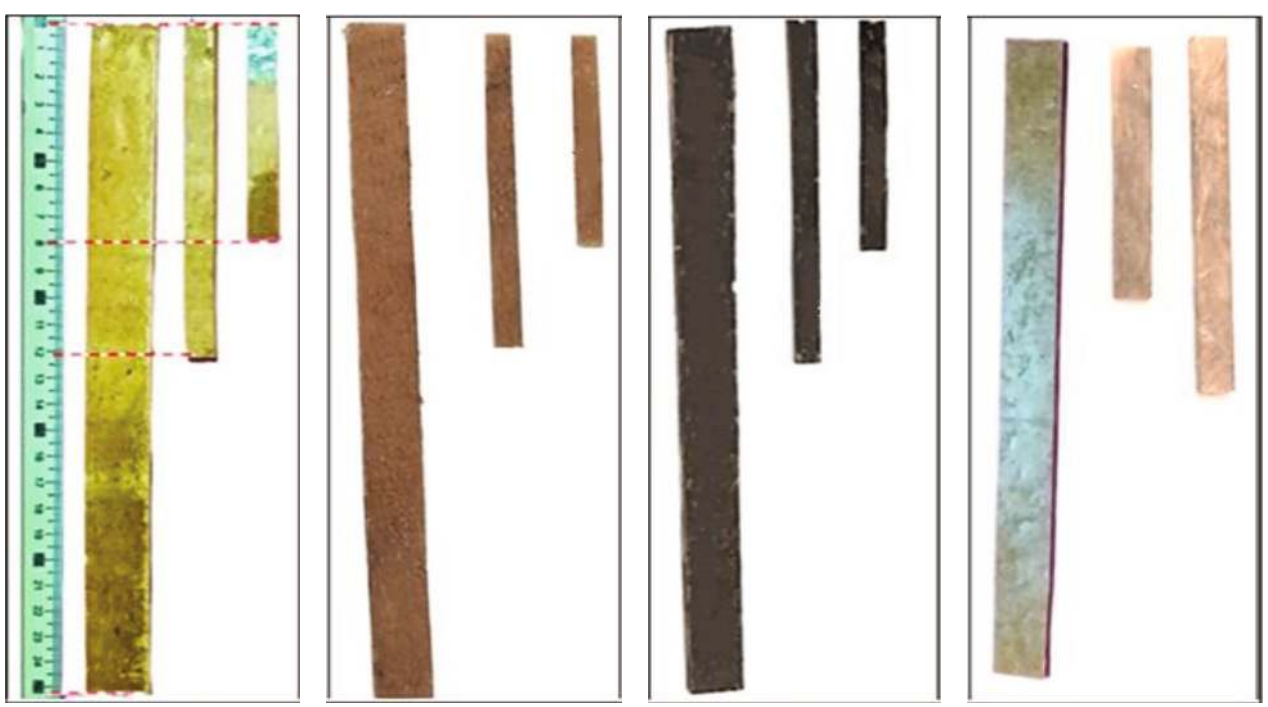


Figure 11: Tensile, compression, and flexural standard specimens of (a) PLAF-WLF, (b) WLF, (c) NWLF, and (d) PLAF composite materials.

Table 3: Water absorption of *Periploca laevigata* Aiton fiber.

Sample	W_1 (g)	W_2 (g)	Water ABS %
1	0.5707	0.6419	11.09
2	0.5641	0.6293	10.36
3	0.5744	0.621	7.50
4	0.5785	0.6247	7.40
5	0.5785	0.6235	7.22

Table 4: The density and void fraction of the specimen samples.

Sample	Td (g/cm^3)	Md (g/cm^3)	V (%)
WLF	1.130	1.092	3.361
NWLF	1.130	1.095	3.095
PLAF-WLF	1.041	1.029	1.182
PLAF	0.887	0.877	1.098

four fiber groups and epoxy resins, have been mechanically tested by tensile, compression, and flexural tests. Accordingly, the next two subsections present and analyze the collected findings of the fiber characterization and mechanical properties of the four composite materials.

4.1. Characterization Results of WLF, NWF, PLAF-WLF, and PLAF Natural Fibers. The structures of all the processed natural fibers were characterized by FTIR, XRD, and SEM tests. First, the FTIR spectroscopy results are presented in Figure 12 and Table 5 which indicate similarities in organic structures and chemical bonding between PLA and wool fibers. The peak around 1519 cm^{-1} in Figure 12 is known as the (-C-N-H) bond's bending deformation peak, and it demonstrates that C-N stretching is closely connected to N-H bending. The peaks at 1585, 1566, 1681, and 1573 cm^{-1} shown in Figures 12(a), 12(b), 12(c), and 12(d) are caused by the -CO stretching bond of the amide group. The peak in Figures 12(a), 12(c), and 12(d) is around 3699–3788 cm^{-1}, while the peak in Figure 12(b) is approximately 3703 cm^{-1}, proving that the water (-OH) in the samples indicates minimal variation in the peaks. The Amide II peak became more evident in the treated samples since its location changed based on the treatment conditions. In Figures 12(b), 12(c), and 12(d), the presence of peaks at 1288, 1276, and 1284 cm^{-1} is indicative of components associated with both α-helical conformation and disordered structure. These spectral features provide insights into the molecular composition and structural characteristics.

Second, the XRD results are shown in Figures 13(a), 13(b), 13(c), and 13(d). Through the two resulting curves shown in Figures 13(c) and 13(d) of untreated *P. laevigata* fiber and of untreated wool fiber, respectively, which record information about the crystal structures present in the studied samples, we notice that the peak corresponding to the angle $2\theta = 25.62^\circ$ in Figure 13(c) is closely related to the peak of the angle $2\theta = 26.67^\circ$ in Figure 13(b). The same observation was recorded through two curves shown in Figure 13(a) of treated wool fiber by 0.1% NaOH and Figure 13(b) of treated wool fiber by cold plasma mixed with untreated *P. laevigata* fiber, which noticed information on the crystal structures found in the samples during the study. We find that the peak corresponding to the angle $2\theta = 20.98^\circ$ in Figure 13(c) is closely related to the peak of the angle $2\theta = 21.39^\circ$ in Figure 13(b). As a result of the two curves shown in Figures 13(a) and 13(b), we conclude that the wool fiber crystallinity is linked to its chemical, physical, and mechanical characteristics. The crystallinity of wool fiber was observed to decrease as a result of alkali treatment. This reduction in crystallinity can likely be attributed to the damage inflicted upon the polypeptide chain during the alkali treatment process. Specifically, due to the decomposition of a portion of the crystal structure, a modest decrease in crystallinity was observed, as confirmed by [51].

Third, SEM was utilized to examine the morphology of the four composites. In Figures 14(a), 14(b), 14(c), and 14(d), SEM micrographs vividly depict the surface characteristics of these specimens. When studying the surface of untreated wool fiber following conventional cleaning, as seen in Figure 14(b), these fibers exhibit prominent scales elevated at the edges, sharp scale structures, and a smooth cuticle layer, owing to the presence of amino acids. Figures 14(a) and 14(d), however, reveal observable alterations in the surface morphology of the chemically treated and cold plasma–treated wood-reinforced composites. Notably, the micrographs illustrate that the chemical treatment has resulted in a reduction of scale edges, indicative of some degree of smoothing or scale removal on the wool-reinforced composites. Conversely, the micrographs indicate that the cold plasma treatment has introduced a degree of roughness on the cuticle surface. For PLAF displayed in Figures 14(c) and 14(d), the presence of a smooth surface suggests that the cuticle layer remains in its raw, untreated, and natural state, without any specific treatment or modification applied. Notably, the SEM images in Figures 14(b) and 14(c) reveal identical cells on the outer layer of untreated wool fiber and untreated PLAF for each species. This shared characteristic holds the potential for enhancing adhesion between the fiber and the resin.

To sum up the findings of the structural characterization of fibers, it can be said that the XRD revealed no variations in crystallinity, showing that plasma treatment caused degradation only on the surface of cellulosic materials [52]. FTIR analysis of the *P. laevigata* fiber revealed a close similarity in organic structures and chemical bonds to wool fiber. This similarity indicates that the two types of fiber share common functional groups and molecular arrangements. The FTIR analysis provides valuable information about the chemical composition and bonding characteristics of the fiber. XRD analysis confirmed the similarity between the fiber structures of *P. laevigata* fiber and wool fiber. The results of XRD analysis indicated that the *P. laevigata* fiber exhibits similar patterns to wool fiber, suggesting similarities in the arrangement of molecules and crystalline structure. The close overlap between wool fiber and *P. laevigata* fiber in terms of their organic structures and chemical bonds contributes to the formation of a hybrid composite (PLAF-WLF) with improved hardness and strength. SEM can

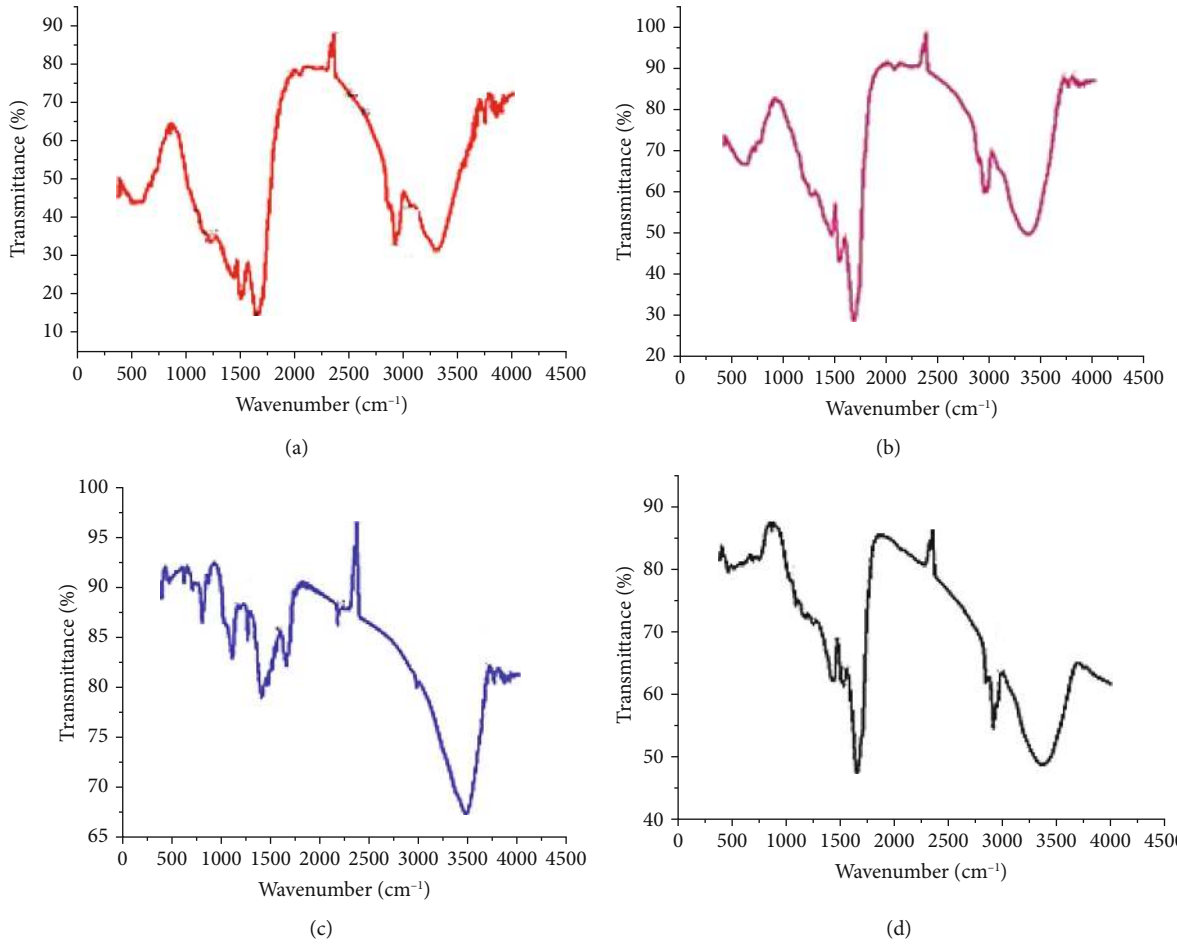


Figure 12: FTIR spectroscopy plots: (a) PLAF-WLF, (b) NWLF, (c) PLAF, and (d) WLF.

Table 5: FTIR spectroscopy results.

Sample	Amide III	Amide I (=C=O)	C–N-H	-OH
Untreated wool fiber	1232 cm^{-1}	1573 cm^{-1}	1519 cm^{-1}	3699–3788 cm^{-1}
Wool treated by NaOH	1288 cm^{-1}	1585 cm^{-1}	1519 cm^{-1}	3699–3788 cm^{-1}
Wool treated by plasma	1276 cm^{-1}	1566 cm^{-1}	1519 cm^{-1}	3703 cm^{-1}
Untreated *Periploca laevigata*	1284 cm^{-1}	1681 cm^{-1}	1519 cm^{-1}	3699–3788 cm^{-1}

indeed reveal the inherent compatibility between *P. laevigata* and wool fiber treated by cold plasma.

4.2. Evaluations of Mechanical Properties for the Four Composite Materials. After the characterization of the fibers, which were processed under different conditions, the fabricated four composites were subjected to three mechanical tests, namely, tensile, compression, and flexural tests, to show the composite's response to different types of loadings. The collected results are presented, analyzed, and discussed in detail, as shown in the below sections.

4.2.1. Tensile Test Results. The tensile test specimens were tested by using a universal tensile test machine to provide them with a set of mechanical properties such as ultimate tensile strength (megapascal), Young's modulus of elasticity (gigapascal), and ductility (percentage). The collected data were plotted in the form of the stress–strain curves.

Figure 15 demonstrates that the tensile stress–strain relations exhibit significantly linear behavior. This is consistent with established theory, particularly regarding mechanical properties in the fiber direction, which are predominantly influenced by fiber properties that maintain a linear stress–strain relationship up to the point of fracture [53]. The hybrid composite PLAF-WLF demonstrated the highest tensile strength of 26.02 MPa, which can be attributed to the effective bonding between the wool fiber and the PLAF within the matrix. This strong bonding was achieved through the vacuum infusion process, and this observation highlights the substantial impact of the stacking sequence

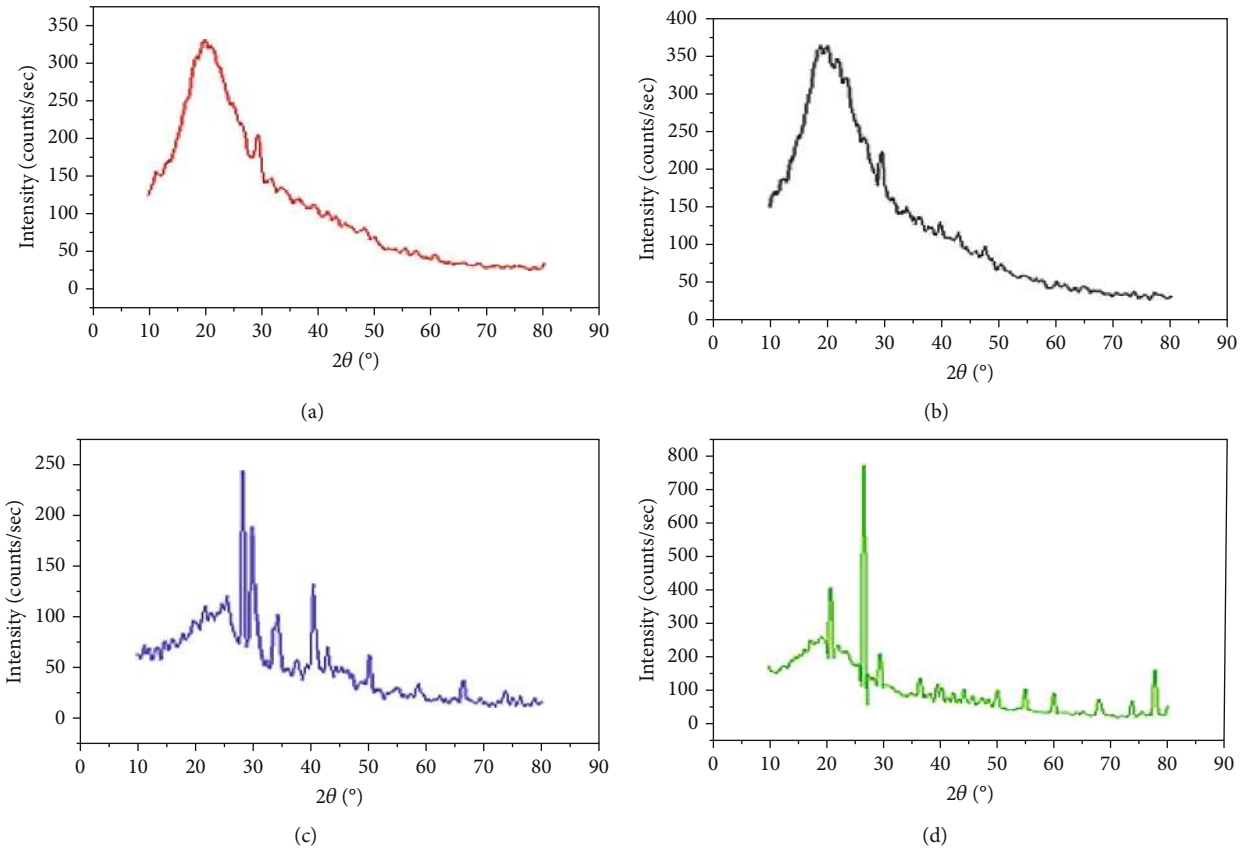


Figure 13: X-ray diffraction pattern: (a) NWLF, (b) PLAF-WLF, (c) PLAF, and (d) WLF.

of reinforcements on the overall properties of the composite [54]. During the test, the composite head endured the maximum amount of stress, which delayed the occurrence of the initial fracture beyond the expected time frame. This delay can be attributed to the fiber's ability to absorb a significant portion of the load, effectively boosting its yield point. However, after a short while, the fiber approaches the necking point, indicating the stage where the material is vulnerable to fracture, leading to crack propagation, which is caused by the damage of the epoxy matrix.

Figures 16 and 17 show the values of the forces and Young's modulus. The composite, consisting of untreated wool fiber, demonstrated a tensile strength of 10.82 MPa and Young's modulus of 1420.34 MPa (1.42 GPa), and the composite treated with 0.1% NaOH exhibited even more impressive mechanical properties, achieving a tensile strength of 13.89 MPa and Young's modulus of 1688.55 MPa (1.688 GPa). In comparison, the composite PLAF stands out with higher mechanical performance, showcasing a remarkable tensile strength of 20.1 MPa and Young's modulus of 2345.73 MPa (2.3457 GPa). However, the hybrid composite PLAF-WLF surpasses them all with an impressive tensile strength of 26.02 MPa and Young's modulus measuring 2350.50 MPa (2.350 GPa). These remarkable results highlight the synergistic effect of cold plasma treatment and the addition of PLAF, yielding a composite with remarkable mechanical properties, making it a compelling choice for applications demanding both strength and stiffness. Untreated wool fiber composite WLF, when not subjected to any treatment, exhibits noticeable accumulations of contaminants visible on their exterior. As previously noted by other researchers, these contaminants present on the surface of the fiber lead to suboptimal bonding between the fiber and the matrix material, primarily because of the restricted contact area between the two components [55]. Weak interfacial bonding leads to the creation of partially isolated microspaces that impede the transfer of stress between the fiber and the matrix, as seen in Figure 18. As the fiber loading increases, the level of obstruction also increases, resulting in heightened stiffness [56]. Following the treatment of wool fiber with 0.1% NaOH, there was an observed improvement in both tensile strength and Young's modulus. This outcome can be analyzed from various perspectives. To begin with, in accordance with the theory of fiber-reinforced polymeric matrices, the overall composite modulus experiences enhancement because the load exerted on the matrix gets effectively transmitted to the fiber during the tensile procedure [57]. The PLAF composite displayed exceptional mechanical performance, and these remarkable mechanical properties are a result of the fiber's inherent qualities and purity. It is worth noting that this plant fiber achieved such performance without any treatment or modification, emphasizing its natural lightweight and thin characteristics.

The incorporation of PLAF into cold plasma–treated wool resulted in a significant improvement in terms of both

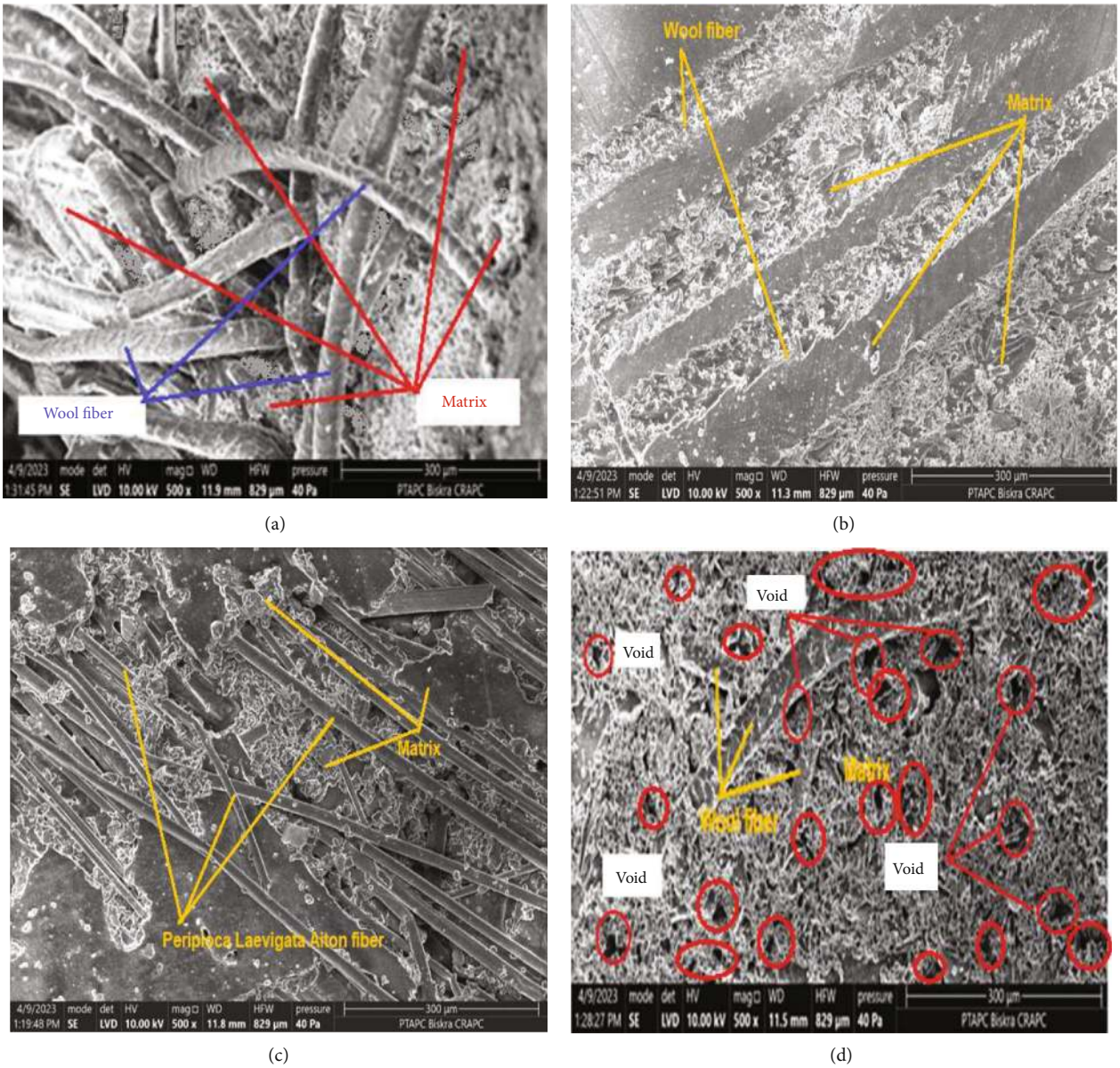


Figure 14: Scanning electron microscopy: (a) PLAF-WLF, (b) NWLF, (c) PLAF, and (d) WLF.

Young's modulus and tensile strength. This improvement can be attributed to the remarkable organic and structural similarities between PLA and wool fibers, despite their distinct natural origins. However, their organic compatibility has been proven by XRD and FTIR analysis. Cold plasma treatment alters the surface properties of wool fiber; it can introduce functional groups and change the surface energy, which can enhance its compatibility with other materials. Depending on the specific treatment parameters, cold plasma can strengthen wool fiber by cross-linking or modifying the fiber's structure, and this can result in improved tensile strength and durability [58]. The modified surface of plasma-treated wool fiber can promote better adhesion to other materials or matrices in composite materials, resulting in improved mechanical properties [59]. The addition of PLAF to WLF results in substantial improvements in tensile strength. Specifically, it leads to a remarkable increase of 58.57% in tensile strength for untreated wool fiber composite WLF, a significant enhancement of 46.62% for NaOH-treated wool fiber composite NWLF, and a notable rise of 22.75% for PLAF composite. This demonstrates the positive impact of incorporating PLAF into the composite, highlighting its potential to significantly enhance the tensile properties of these materials, especially for untreated and NaOH-treated wool fiber. It leads to significant improvements in Young's modulus; impressively, it leads to a substantial 39.57% increase in Young's modulus for WLF and a noteworthy 28.16% improvement for NWLF composite. However, the effect is negligible, increasing for PLAF composite. This indicates that PLAF played a significant role in bearing a considerable percentage of the applied stress force on the sample. It underscores the positive impact of incorporating PLAF into the composite, highlighting their potential to significantly enhance the tensile properties of

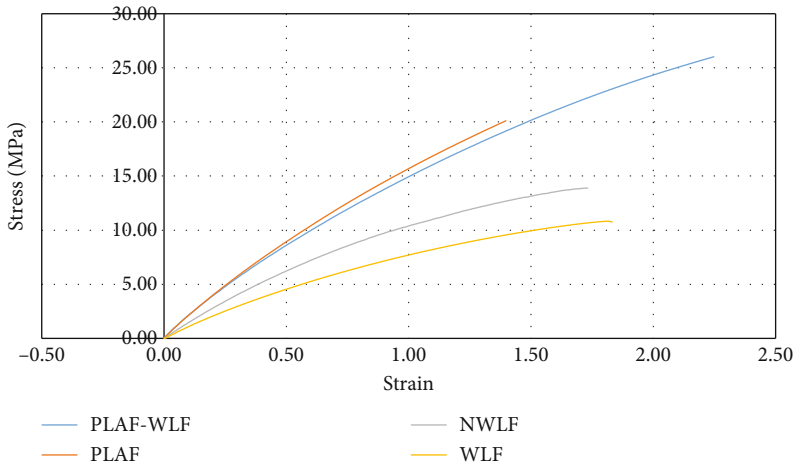


Figure 15: Stress versus strain curves for tensile test.

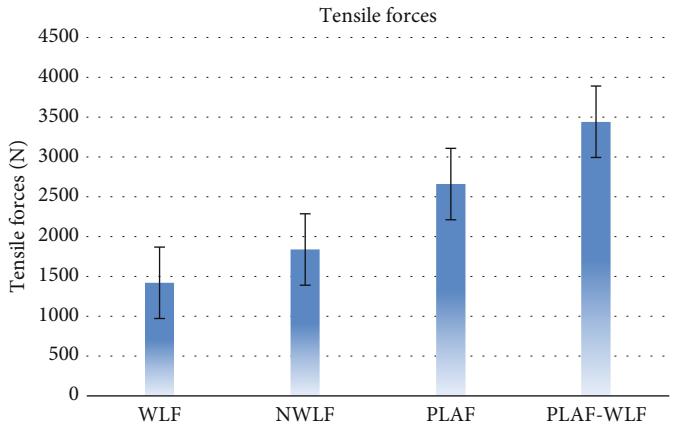


Figure 16: Tensile test forces.

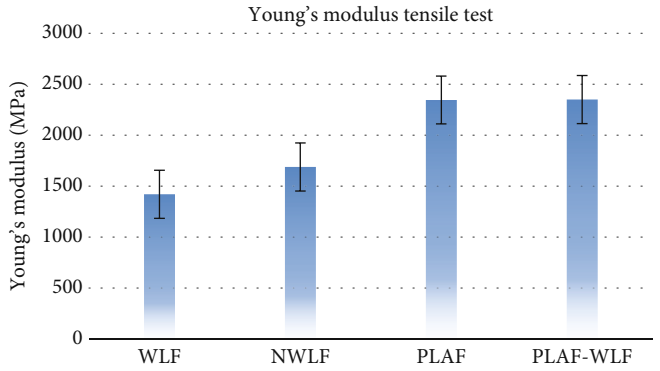


Figure 17: Young's modulus tensile test.

these materials, particularly in the case of WLF and NWLF composites. Young's modulus is remarkably high, with a value of 2.35 GPa. This indicates that the composite is rigid and shows great resistance to deformation under load. The tensile strength is also large, at 26.02 MPa. Indeed, the substantial increase in both Young's modulus and tensile strength in the composite material indicates its ability to withstand significant tensile stress without breaking. This correlation between these two material characteristics underscores its strength and durability.

Macro- and microphotographs were utilized to assess the fractures in the tensile test specimens and identify the



Figure 18: Optical microscope image of microscope image of untreated wool fiber indicates the presence of the impurities.

features of the tensile test results. Figures 19(a), 19(b), 19(c), and 19(d) exhibit macroimages of the fracture in a tensile test specimen.

Figures 20(a), 20(b), 20(c), and 20(d) display the various types of tensile fracture observed in WLF, NWLF, PLAF-WLF, and PLAF specimens, respectively, at microscopic scales. Fiber pullout is a common failure mechanism in NWLF and WLF specimens, indicating inadequate adhesion of the matrix to the fibers. The fracture structure of the PLAF-WLF composite, depicted in Figure 20(c), does not exhibit interlaminar cracks, confirming satisfactory adhesive strength. Additionally, the fractured structure shows minimal defects like microspores and fiber elongation, suggesting the potential for enhancing mechanical properties through process optimization [5]. Fracture-type analysis demonstrates that the hybridization of wool fibers and PLAFs contributes to improved interlaminar properties and increased mechanical strength.

Table 6 demonstrates a comparison between the results and those of alternative composite materials that utilize natural fibers for reinforcement.

4.3. Flexural Test. The flexural test examines the response of the beam specimen to the bending loading and determines its flexural strength and flexural modulus. The test was carried out according to the ASTM D790 standard. The achieved data was plotted in the stress–strain and force-displacement forms.

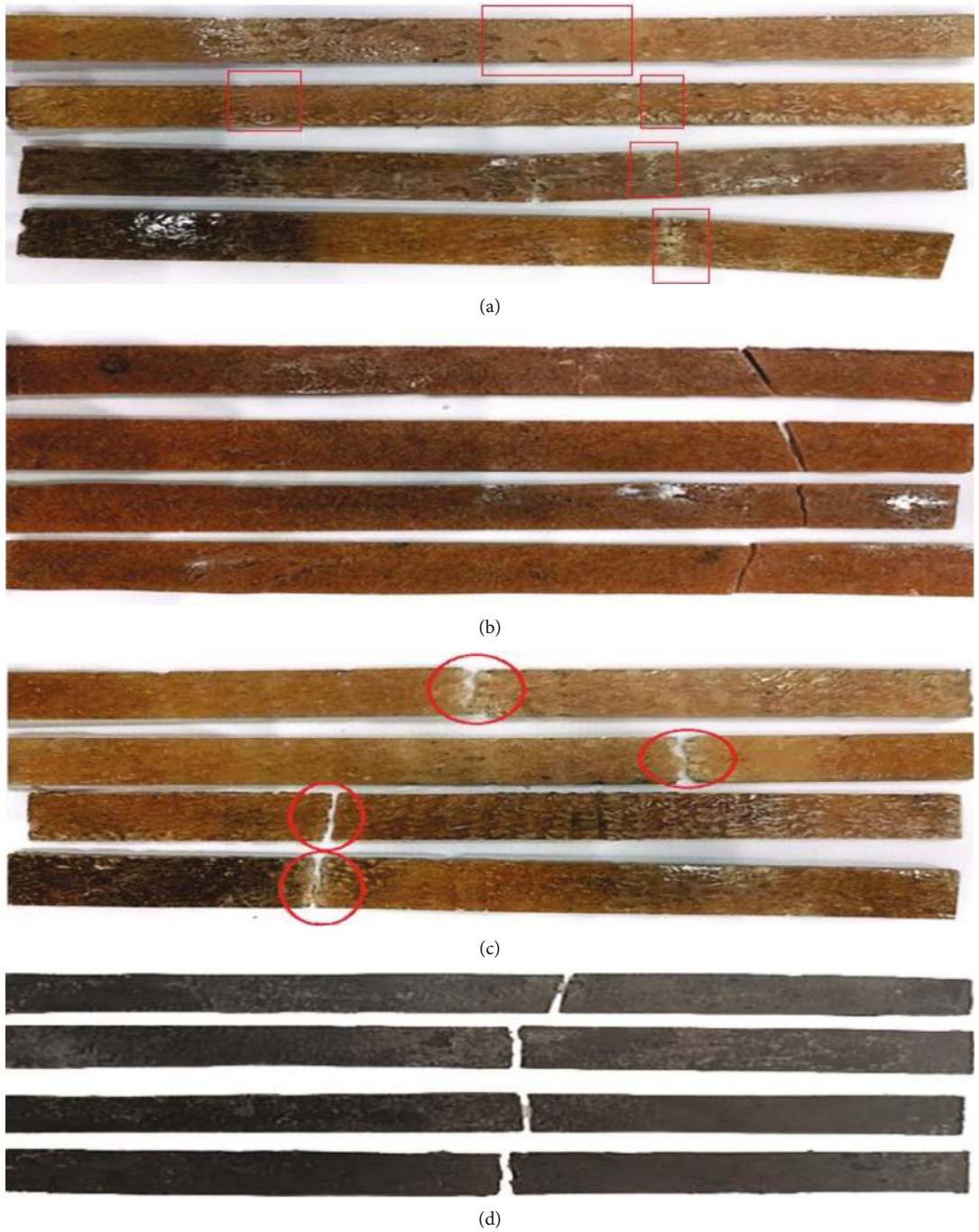
Figure 21 shows the flexural strength values for the four composites. Notably, the PLAF-WLF composite exhibits a higher flexural strength compared to the other composites. In terms of deflection, the WLF composite was found to have the maximum deflection, followed by the NWLF composite, among the hybrid composites investigated in the study. The results of the flexural test, as illustrated in Figure 21, demonstrate the remarkable performance of the hybrid composite PLAF-WLF. It exhibits a notable 72.70% increase in flexural strength compared to WLF composite, aligning with expectations due to the inherent higher flexural strength of PLAF when combined with plasma-treated wool fiber. Furthermore, the hybrid composite PLAF-WLF surpasses the NWLF composite by a substantial 67.84% and even outperforms the PLAF composite by 56.03%. These findings underscore the synergistic effect achieved by integrating WLF with PLAF, resulting in a composite material with exceptional resistance to flexural forces. Figures 22, 23, and 24 show the mechanical properties of composite materials under applied forces. Notably, the hybrid composite PLAF-WLF emerges as a standout candidate, displaying exceptional strength by withstanding a peak force of 253.15 N and boasting Young's modulus of 1210.93 MPa (1.21 GPa). This outstanding performance surpasses that of all other materials examined. Additionally, PLAF composite, derived from PLAF, demonstrates significant strength, recording a force of 111.29 N and Young's modulus of 623.2 MPa (0.6223 GPa). Furthermore, the NWLF composite exhibited a force value of 81.39 N, accompanied by Young's modulus of 588.5 MPa (0.588 GPa), highlighting the beneficial effects of chemical treatment on their mechanical properties. Conversely, the WLF composite exhibited the lowest force values at 69.09 N, coupled with Young's modulus of 524.83 MPa (0.524 GPa), underscoring the importance of treatment processes in enhancing material characteristics. These findings unequivocally underscore the remarkable and advantageous impact achieved through the amalgamation of PLA and wool fiber, particularly when the latter undergoes cold plasma treatment within the hybrid composite, promising innovations in material engineering and applications.

Figure 23 illustrates that the hybrid composite PLAF-WLF exhibits greater flexibility when compared to another composite. In contrast to both NWLF and PLAF composites, the WLF composites display a brittle nature and are incapable of withstanding significant flexural loads. When bending forces are exerted on a composite, the fiber located on the outer surface experiences higher levels of stress. The effective penetration of resin into the fiber, which contributes to flexural strength, depends significantly on the adhesive properties between the fiber and the matrix. It has also been noted that hybridizing natural fiber tends to enhance flexural strength compared to using single fiber alone [54].

Figures 25(a) and 25(b) show PLAFs and wool fibers under an optical electron microscope. The pure structural nature and low density of *Periploca laevigata* fibers, not subjecting them to any physical or chemical treatments, gave the composite remarkable stiffness and low elongation, which enhanced the bending strength and flexural Young's modulus of the PLAF.

Wool fiber has different functional groups like hydroxyl (-OH), amino (-NH2), amide (-CONH-), and carboxyl (-COOH) groups [49]. The O-H and C-OOH groups on the fiber surface are exposed when waxy substances dissolve, resulting in increased polarity and decreased acidity of the fiber's surface topography. Surface functional groups are linked by interactions between energized plasma species and the substrate surface, whereas surface bridges are typically created by reactions between excited surface species [63].

Effective penetration of the resin into the fibers contributes to the strength of the flexural test and affects the adhesion properties between the fibers and the matrix. Hybridization of natural fibers tends to enhance flexural



(a)

(b)

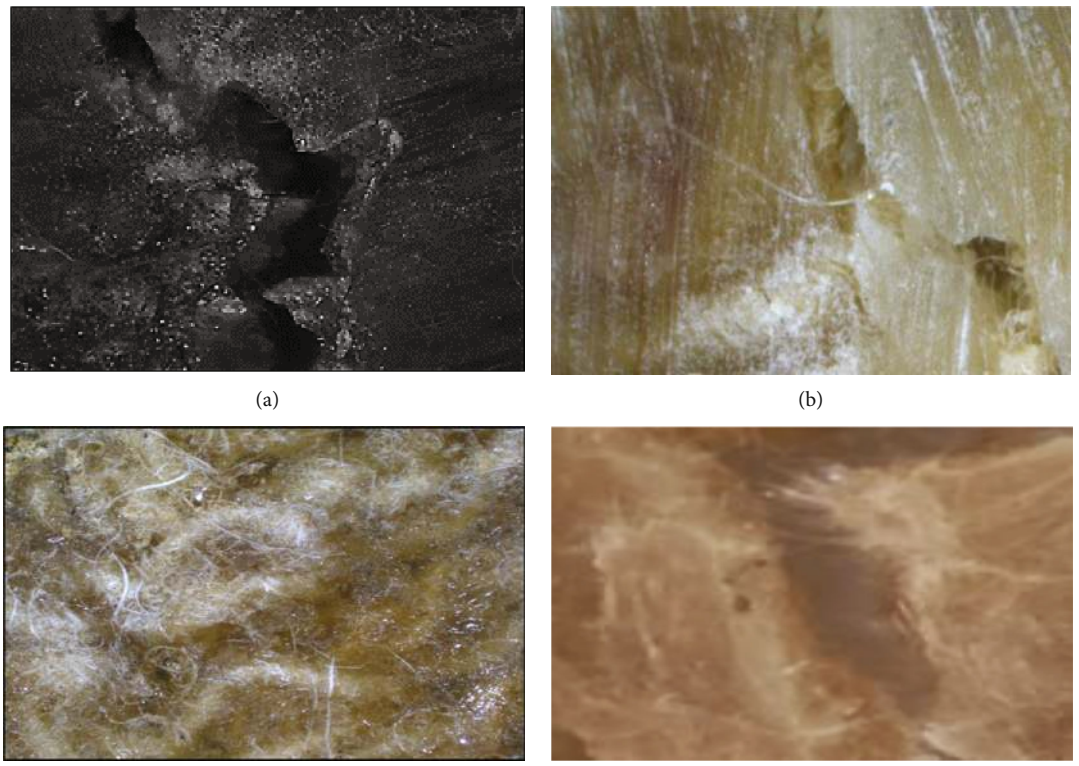
(c)

(d)

Figure 19: Specimens after the tensile test.

strength compared to using single fibers alone [54]. The results depicted in Figures 26(a), 26(b), 26(c), and 26(d) from bending tests of PLAF-WLF, NWLF, PALF, and WLF, respectively, demonstrate that incorporating *Periploca* into wool fibers enhances their capacity to bend without fracturing. This indicates that the inclusion of these fibers boosts ductility. Following an examination of the failure mode exhibited by the specimens in bending tests, it was conclusively determined that the addition of *Periploca* fibers to the composite hybrid effectively altered the brittle behavior of untreated wool fibers under concentrated loading to a more ductile failure mode. As a result, the incorporation of *Periploca* fibers into wool fibers facilitates the transmission of tensile stress along the sample axis, ultimately increasing the ductility of the hybrid composite.

4.4. Compression Test Results. The mechanical performance of the four composites was additionally evaluated when they were subjected to another type of mechanical test represented by the compression test. In this test, all specimens were subjected to compressive stress to show their response to this type of loading.



(a) (b) (c) (d)

Figure 20: Tensile fracture specimen of NWLF, WLF, PLAF, and PLAF.

Table 6: The tensile strength and modulus of the current study with some literatures of different composites.

Composites	Description	Young's modulus (GPa)	Tensile strength (MPa)	References
KRFP (90° D)	Kenaf with fiber orientation of 90°	0.33	3.52	[60]
KRFP (0° D)	Kenaf with fiber orientation of 0°	2.43	42.38	
HYBRID CKFRP (90° D)	Hybridization of carbon kenaf with fiber orientation of 90°	3.43	43.11	
H	Composite laminate RFFFR (ramie/3 layer of flax/ramie)	0.98	54	[54]
G	Composite laminate FRRRF (flax/3 layer of ramie/flax)	0.96	39.08	
HH/PLA	Horsehair fiber-based polylactic acid	4.52	30.33	[61]
Untreated luffa	Untreated luffa fiber	2.37	11.43	[62]
Treated luffa	Treated using benzoyl chloride and NaOH	3.54	14.54	
S10	Coconut fiber treated with KOH and polypropylene	1.03	23.17	[60]
S2	Coconut fiber treated with KOH and polypropylene compositions	0.62	21.76	
PLAF-WLF	*Periploca laevigata* Aiton fiber/wool fiber treated by cold plasma	2.35	26.02	
PLAF	*Periploca laevigata* Aiton fiber	2.34	20.1	
NWLF	Wool fiber treated with NaOH	1.688	13.89	
WLF	Untreated wool fiber	1.42	10.82	

Figures 27 and 28 demonstrate the compressive strength and Young's modulus of the PLAF composite, characterized by its noteworthy Young's modulus of 500 MPa (0.5 GPa) and compressive strength of 44.75 MPa. Despite not having the highest load-bearing capacity among the tested materials at 2755.19 N, PLAF composite still displays substantial

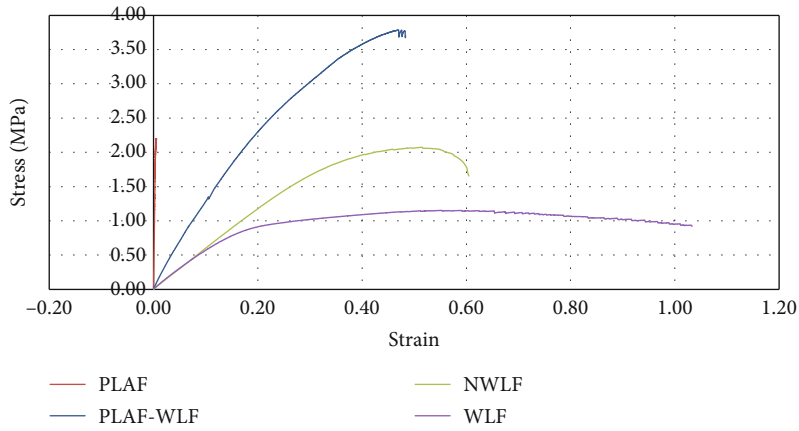


Figure 21: Stress versus strain curves for the flexural test.

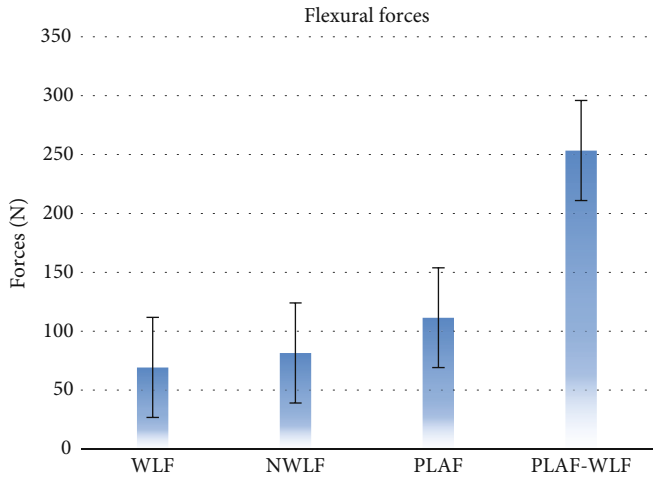


Figure 22: The flexural test forces.

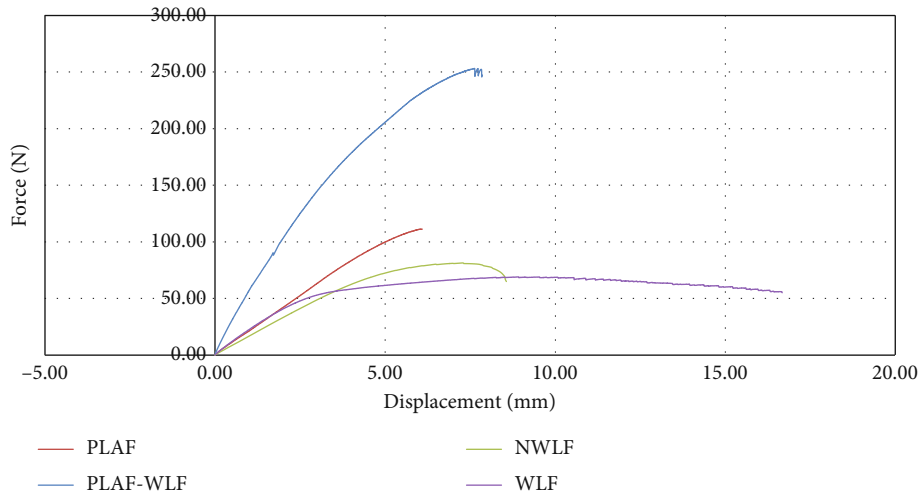


Figure 23: Force versus displacement curves.

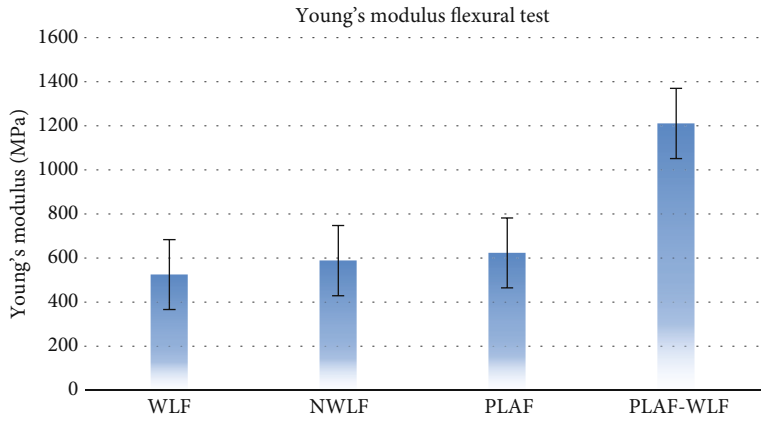
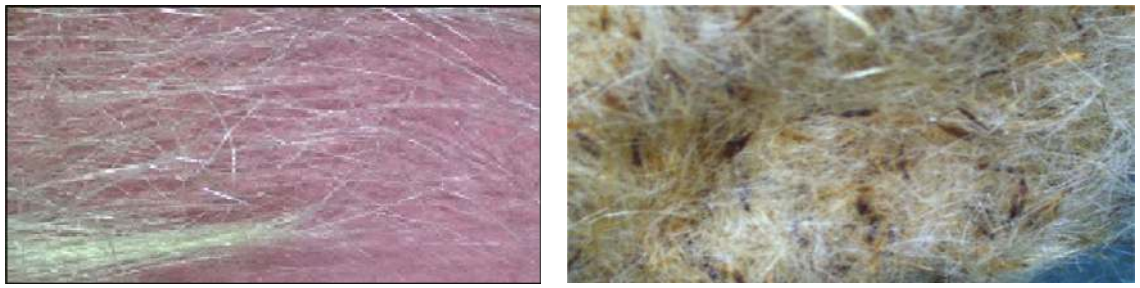
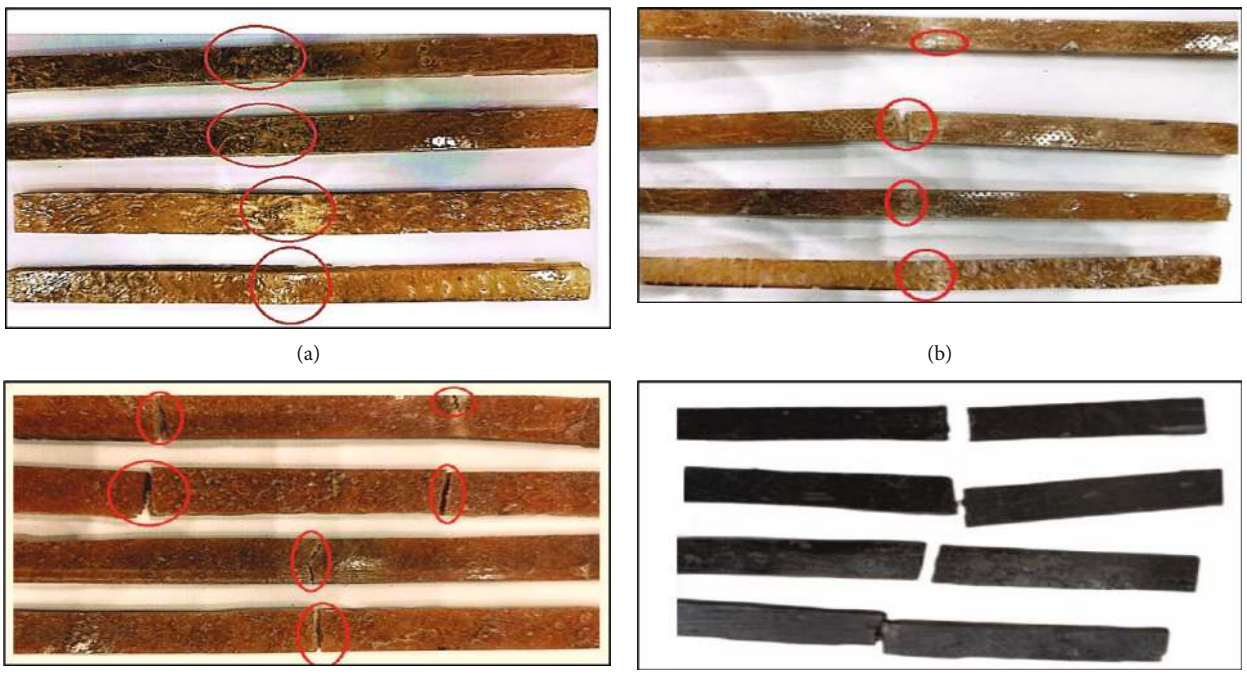


Figure 24: Young's modulus flexural test.



(a) (b)

Figure 25: (a) *Periploca laevigata* Aiton fibers and (b) wool fibers under an optical electron microscope.



(a) (b)

(c) (d)

Figure 26: The specimens of composites: PLAF-WLF, NWLF, PALF, and WLF after the flexural test.

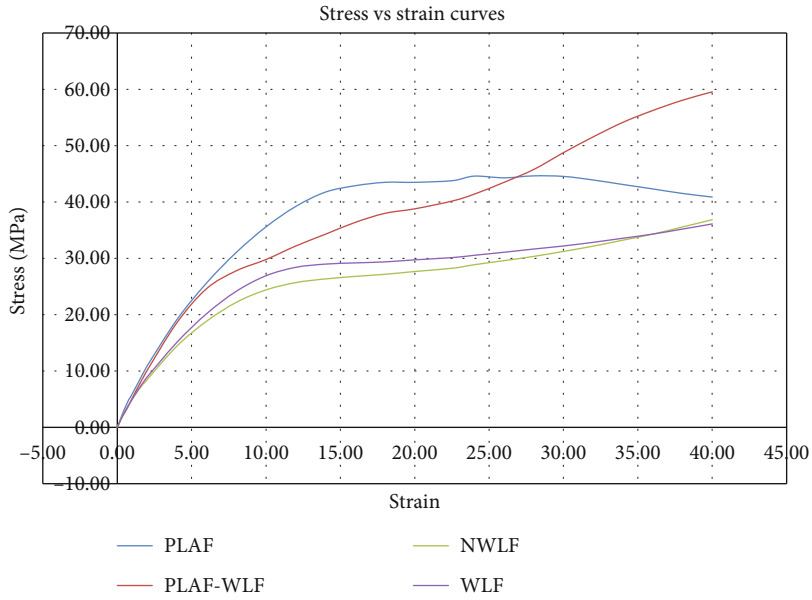


Figure 27: Stress versus strain curves for the compressive test.

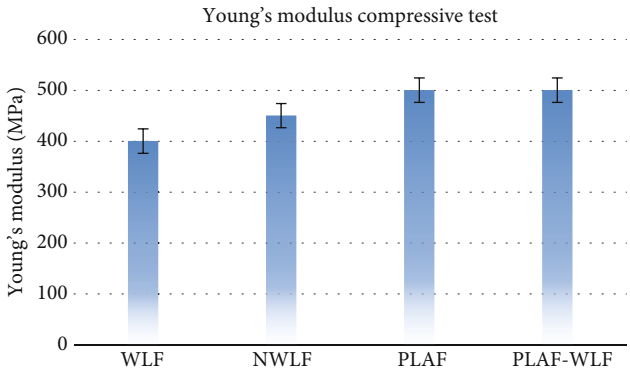


Figure 28: Young's modulus compressive test.

strength and rigidity. PLAF-WLF, a hybrid, demonstrates exceptional mechanical properties. With a load-bearing capacity of 4369.19 N, it achieved the highest compressive strength of 59.56 MPa among all tested specimens. Furthermore, its Young's modulus measures an impressive 500 MPa (0.5 GPa), highlighting its remarkable stiffness. NWL composite displays a load-bearing capacity, achieving a load measurement of 1829.25 N, and it possesses Young's modulus of 450 MPa (0.45 GPa) and compressive strength of 36.87 MPa. This marked improvement in strength compared to untreated wool composite WLF strongly indicates that the NaOH treatment has effectively reinforced the material. WLF composite, comprising untreated wool fiber, displays the lowest load value among the tested materials, with a load measurement of 1134.18 N. Furthermore, it has Young's modulus of 0.4 GPa and compressive strength of 36.12 MPa. These results emphasize the importance of fiber treatment or modification to enhance its load-bearing capacity, as demonstrated by the improvements seen in NaOH-treated wool fiber composite NWL and hybrid composite PLAF-WLF when compared to the untreated wool fiber composite WLF. The compressive strength results reveal significant variations in the performance of different composites.

The hybrid composite achieved the highest compressive strength at 59.56 MPa, while the WLF composite exhibited the lowest at 36.12 MPa. Interestingly, the PLAF composite, with a fiber/epoxy ratio of 17.65%, achieved a compressive strength of 44.76 MPa. In contrast, the PLAF-WLF composite, with a fiber/epoxy ratio of 14.29% PLAF and 28.57% treated wool fiber through cold plasma, reached the same impressive compressive strength as the hybrid composite at 59.56 MPa. Finally, the NWLF and WLF composites, both with a high wool fiber/epoxy ratio of 42.86%, achieved compressive strengths of 36.87 and 36.12 MPa, respectively. These results unequivocally demonstrate that the inclusion of PLAF provides substantial additional strength and stiffness to the wool fiber. Notably, the compressive strength of the wool fiber composite increased by approximately 39.35% due to the synergistic effect of incorporating PLAF. In a comparative analysis of mechanical properties, PLAF composite stands out as a superior material when compared to WLF composite, showcasing a remarkable 19.30% higher load-bearing capacity and an astonishing 20% greater Young's modulus, underscoring its exceptional strength and stiffness. Additionally, the hybrid composite PLAF-WLF displays an impressive 38.09% increase in load-bearing capacity over pure NWLF composite, highlighting its exceptional strength, although it does involve a slight compromise in stiffness.

It confirms the successful integration of the fiber and supports the enhanced interfacial bonding and overall performance of the composite material. Four composite materials were created in this study, including a composite with PLAF. This composite consists of a PLAF and is used as the reinforcing component. The PLAFs are likely in their

untreated form and provide their inherent properties to the composite. A hybrid composite with wool fiber treated by cold plasma mixed with untreated PLAF (PLAF-WLF). In this composite, wool fibers are treated with cold plasma to improve their properties. The treated wool fibers were then combined with untreated *P. laevigata* fiber to create a hybrid composite material. The reinforcing component is untreated wool fiber. The wool fibers are used in their natural state without any additional treatment or modification. A composite with wool fiber treated chemically with 0.1% NaOH (NWLF) involves treating wool fiber chemically with a 0.1% solution of NaOH. The analysis was conducted for both treated (NaOH and plasma) and untreated fiber, revealing a decrease in fiber adhesion rates compared to untreated fiber. In the single composites, PLAF comprised 20% of the total weight, WLF accounted for 30%, and the remaining 70% was epoxy. In the hybrid composite (PLAF-WLF), PLA contributed 10%, wool contributed 20%, and epoxy made up the remaining 70%. Notably, in the PLAF and WLF composites, epoxy constituted 80% and 70% of the total weight, respectively. The mechanical behavior, including tensile, compressive, and flexural strength, of both single and hybrid composites was investigated in accordance with ASTM standards. The hybrid composite, PLAF-WLF, demonstrated superior mechanical properties under loading conditions as compared to the single fiber-reinforced composites (PLAF, WLF, and NWLF). The introduction of PLAF had a substantial positive impact on the tensile properties of composites. Table 6 shows the percentages of voids during the manufacturing process that may introduce defects in the composite, such as microvoids in the matrix. These imperfections can lead to localized stress concentration, ultimately causing potential failure. During compression, the composite characteristics are influenced by the quality of the fiber-matrix interface and the stiffness of the resin. A stiffer matrix offers improved lateral support to the fiber, thereby delaying fiber microbuckling and enhancing the strain to failure [64].

The vacuum infusion molding process was used in this study to manufacture composite material. This process can solve challenges with manual lay-up and spray-up methods. The vacuum infusion molding process eliminates the risk of trapped air in the composite, and this process enables the composite to be manufactured in repetition with the same purity because it is dependent on the design of the equipment rather than the operator's competence [43].

Based on the obtained mechanical properties, it can be said that one of the most compelling aspects of PLAF composites is their compatibility with hybridization, particularly when combined with wool fiber. This synergy results in significant enhancements across various mechanical properties, including tensile strength, Young's modulus, compressive strength, and flexural strength. This adaptability makes it a versatile choice for industries aiming to boost performance while maintaining a lightweight profile.

To sum up, the introduction of PLAF into composite materials represents a promising leap in materials engineering. It offers a lightweight, robust, and versatile alternative that has the potential to revolutionize a wide range of industries.

5. Conclusions

The study focused on evaluating the effect of hybridization on the properties of the resulting materials, with the aim of understanding how different fiber blends affect the overall performance of composites. The experimental approach allowed a detailed analysis of the mechanical and structural properties of the hybrid composites. The following conclusions can be drawn:

- The hybrid composite exhibits tensile, flexural, and compressive strengths, measuring 26.02 MPa, 2.53 GPa, and 109.22 MPa, respectively. In addition, it has Young's modulus of 2.35, 1.21, and 0.50 GPa, respectively.
- These results indicate that hybrid composites reinforced with wool and PLAFs have the potential to serve as viable alternative materials, providing significant structural strength for various engineering purposes.
- The combination of PLAFs and WLF provides a pioneering solution for the development of hybrid composites. This innovative technology offers many advantages, making it a valuable choice for diverse applications.
- It is worth noting that PLAFs exhibit an exceptionally low density property, measuring 0.45 g/cm^3.
- In tensile tests, these fibers showed Young's modulus value of 2.345 GPa, indicating exceptional stiffness and resistance to deformation. Furthermore, the PLAF composite showed a flexural strength of 15.58 MPa, displaying its ability to withstand bending forces, and a compressive strength of 12.5 MPa, highlighting its durability under compression.
- These outstanding properties make PLAF composites very attractive to industries that prioritize long-term structural strength and durability. It is worth noting that *P. laevigata* also possesses antibacterial and antioxidant properties, which increases its biological appeal and the possibility of introducing this fiber into several engineering fields.

6. Limitations and Scope for Further Research

The limitations and scope for further research are illustrated in the following points:

- Discover the diverse range of potential uses for *P. laevigata* fiber epoxy composites that extend beyond structural applications.
- Explore the potential of hybridizing *P. laevigata* fiber epoxy composites with other reinforcing materials (carbon fiber, glass fiber, and aramid fiber) to enhance their impact resistance and toughness.

- Investigate the effect of fiber architecture (unidirectional, woven, and random) on the impact resistance of *P. laevigata* fiber epoxy composites.
- Evaluate the impact resistance of *P. laevigata* fiber epoxy composites.
- Conduct comprehensive corrosion resistance testing of *P. laevigata* fiber epoxy composites in different corrosive environments.
- Investigate the susceptibility of *P. laevigata* fiber epoxy composites to bacterial growth, biofilm formation, and biofouling in marine, industrial, and biomedical environments.

Data Availability Statement

The data that support the findings of the study are available from the corresponding author upon request.

Conflicts of Interest

The authors declare no conflicts of interest.

Author Contributions

Conceptualization: Lalmi Rahmani, Mohammed Taher Gherbi, and Aribi Chouaib. Methodology: Lalmi Rahmani, Mohammed Taher Gherbi, and Aribi Chouaib. Experimental: Lalmi Rahmani, Mohammed Taher Gherbi, and Aribi Chouaib. Validation: Lalmi Rahmani, Mohammed Taher Gherbi, and Aribi Chouaib. Formal analysis: Salah Al-Zubaidi. Investigation: H.S.S. Aljibori and M.N. Mohammed. Resources: Lalmi Rahmani, Mohammed Taher Gherbi, and Aribi Chouaib. Data curation: Oday I. Abdullah and Mohammed Fouad Ferhat. Writing–original draft preparation: Lalmi Rahmani, Mohammed Taher Gherbi, and Aribi Chouaib. Writing–review and editing: Salah Al-Zubaidi. Visualization: Salah Al-Zubaidi. Supervision: Oday I. Abdullah. Project administration: Salah Al-Zubaidi and Oday I. Abdullah. Funding acquisition: M.N. Mohammed. All authors have read and agreed to the published version of the manuscript.

Funding

The authors received no specific funding for this work.

References

[1] P. Prabhu, K. Balakrishnan, R. Vannan, and B. Alagappan, "Dynamic mechanical analysis of silk and glass (S/G/S)/pineapple and glass (P/G/P)/flax and glass (F/G/F) reinforced Lannea coromandelica blender hybrid nano composites," *Journal of Materials Research and Technology*, vol. 15, pp. 2484–2496, 2021.

[2] P. Prabhu, V. Chokkalingam, S. Arunkumar, and P. Perumal, "The investigation on mechanical, thermal conductivity and water absorption characteristics of coir fiber-reinforced vinyl ester biocomposites," *Biomass Conversion and Biorefinery*, pp. 1–11, 2024.

[3] R. Payal, "Chapter 9 - Green composites: versatile uses and applications in life," in *Green Sustainable Process for Chemical and Environmental Engineering and Science*, T. Altalhi and Inamuddin, Eds., pp. 165–193, Elsevier, 2022.

[4] W. Ghori, N. Saba, M. Jawaid, and M. Asim, "A review on date palm (phoenix dactylifera) fibers and its polymer composites," *IOP Conference Series: Materials Science and Engineering*, vol. 368, no. 1, article 012009, 2018.

[5] P. Prabhu, A. Balaji, D. Jayabalakrishnan et al., "Study on machining parameters and mechanical properties of hybrid Agave sisalana and glass fiber-reinforced polyester composites (A/GFRP)," *Journal of Natural Fibers*, vol. 19, no. 15, pp. 11644–11657, 2022.

[6] S. Hosseini, M. Gaff, and D. Hui, "Effect of fiber treatment on physical and mechanical properties of natural fiber-reinforced composites: a review," *Reviews on Advanced Materials Science*, vol. 62, no. 1, 2023.

[7] S. Mishra and V. Chaudhary, "Chemical treatment of reinforced fibers used for bio composite: a review," in *Advances in Engineering Materials*, Lecture Notes in Mechanical Engineering, B. P. Sharma, G. S. Rao, S. Gupta, P. Gupta, and A. Prasad, Eds., Springer, Singapore, 2021.

[8] P. Prabhu, K. Balakrishnan, R. Malar Vannan, and B. Alagappan, "Mechanical, thermal and morphological analysis of hybrid natural and glass fiber-reinforced hybrid resin nanocomposites," *Biomass Conversion and Biorefinery*, vol. 14, pp. 4941–4955, 2022.

[9] K. K. Guduru, R. Pandu, S. Banothu, and K. Vinaya, "Synthesis and analysis of natural fibers reinforcement of synthetic resins," *Journal of Material Sciences & Engineering*, vol. 5, no. 5, 2016.

[10] A. Lakshmanan, "Physical and chemical properties of wool fibers," in *Wool Fiber Reinforced Polymer Composites*, pp. 49–71, Woodhead Publishing, 2022.

[11] D. Starovoytova, "Wool grease recovery from scouring effluent at textile mill," *Journal of Agriculture, Pure and Applied Science and Technology*, vol. 10, pp. 1–9, 2014.

[12] P. Zito, M. Sajeva, M. Bruno, S. Rosselli, A. Maggio, and F. Senatore, "Essential oils composition of *Periploca laevigata* Aiton subsp. *angustifolia* (Labill.) Markgraf (Apocynaceae–Periplocoideae)," *Natural Product Research*, vol. 27, no. 3, pp. 255–265, 2013.

[13] K. Rohit and S. Dixit, "A review-future aspect of natural fiber reinforced composite," *Polymers from Renewable Resources*, vol. 7, no. 2, pp. 43–59, 2016.

[14] S. H. Bahrain, N. R. Masdek, J. Mahmud et al., "Morphological, physical, and mechanical properties of sugar-palm (*Arenga pinnata* (*Wurmb*) *merr.*)-reinforced silicone rubber biocomposites," *Materials*, vol. 15, no. 12, p. 4062, 2022.

[15] S. H. K. Bahrain, N. N. C. A. Rahim, J. Mahmud et al., "Hyperelastic properties of bamboo cellulosic fibre–reinforced silicone rubber biocomposites via compression test," *International Journal of Molecular Sciences*, vol. 23, no. 11, p. 6338, 2022.

[16] M. Abdulrazaq Alshekhly, S. Al-Zubaidi, and S. Kamarul Bahrain, "State-of-the-art review of green composites for automotive applications," in *Biocomposite and Synthetic Composites for Automotive Applications*, pp. 347–375, Woodhead Publishing, 2021.

[17] M. K. Ryszard, M. T. Maria, M. Malgorzata, and B. B. Jorge, "Future of natural fibers, their coexistence and competition

with man-made fibers in 21st century," *Molecular Crystals and Liquid Crystals*, vol. 556, no. 1, pp. 200–222, 2012.

[18] G. S. Mann, N. Azum, A. Khan et al., "Green composites based on animal fiber and their applications for a sustainable future," *Polymers*, vol. 15, no. 3, p. 601, 2023.

[19] J. Zach, A. Korjenic, V. Petránek, J. Hroudová, and T. Bednar, "Performance evaluation and research of alternative thermal insulations based on sheep wool," *Energy and Buildings*, vol. 49, pp. 246–253, 2012.

[20] Y. G. Thyavihalli Girijappa, S. Mavinkere Rangappa, J. Parameswaranpillai, and S. Siengchin, "Natural fibers as sustainable and renewable resource for development of eco-friendly composites: a comprehensive review," *Frontiers in Materials*, vol. 6, p. 226, 2019.

[21] K. Al-Kaabi, A. Al-Khanbashi, and A. Hammami, "Natural fiber reinforced composites from date palm fibers," in *11th European Conference on Composite Materials*, Greece: Rhodes, 2004.

[22] U. Soykan, "Development of turkey feather fiber-filled thermoplastic polyurethane composites: thermal, mechanical, water-uptake, and morphological characterizations," *Journal of Composite Materials*, vol. 56, no. 2, pp. 339–355, 2022.

[23] K. S. Meenalochani and V. V. G. Reddy, "A review on water absorption behavior and its effect on mechanical properties of natural fibre reinforced composites," *International Journal of Innovative Research in Advanced Engineering (IJIRAE)*, vol. 4, no. 4, 2017.

[24] K. C. Benini, H. Voorwald, and M. O. Cioffi, "Manufacturing and characterization of high impact polystyrene (HIPS) reinforced with treated sugarcane bagasse," *Journal of Research Updates in Polymer Science*, vol. 6, no. 1, pp. 2–11, 2017.

[25] F. M. Al-Oqla and M. S. Salit, "Natural fiber composites," in *Materials Selection for Natural Fiber Composites*, F. M. Al-Oqla and M. S. Salit, Eds., pp. 23–48, Woodhead Publishing, 2017.

[26] J. Manivannan, S. Rajesh, K. Mayandi et al., "Animal fiber characterization and fiber loading effect on mechanical behaviors of sheep wool fiber reinforced polyester composites," *Journal of Natural Fibers*, vol. 19, no. 11, pp. 4007–4023, 2022.

[27] M. Kulkarni, V. Gavande, P. Mahanwar et al., "Review on biomass sheep wool–based polymer composites," *Biomass Conversion and Biorefinery*, pp. 1–22, 2023.

[28] P. Zito, M. Sajeva, M. Bruno et al., "Essential oil composition of the fruits of Periploca laevigata Aiton subsp angustifolia (Labill.) Markgraf (Apocynaceae-Periplocoideae)," *Natural Product Research*, vol. 25, no. 14, pp. 1339–1346, 2011.

[29] S. Mezhoud, H. Aissaoui, S. Derbré et al., "Flavonoid glycosides from Periploca laevigata (Asclepiadaceae) from Algeria," *Der Pharma Chemica*, vol. 8, pp. 129–131, 2016.

[30] M. Saxena, A. Pappu, A. Sharma, R. Haque, and S. Wankhede, *Composite Materials from Natural Resources: Recent Trends and Future Potentials*, IntechOpen, 2011.

[31] F. Allafi, M. S. Hossain, J. Lalung et al., "Advancements in applications of natural wool fiber: review," *Journal of Natural Fibers*, vol. 19, no. 2, pp. 497–512, 2022.

[32] O. P. Balogun, A. A. Adediran, J. A. Omotoyinbo, K. K. Alaneme, and I. O. Oladele, "Evaluation of water diffusion mechanism on mechanical properties of polypropylene composites," *International Journal of Polymer Science*, vol. 2020, Article ID 8865748, 12 pages, 2020.

[33] M. Arsyad, "Sodium hydroxide and potassium permanganate treatment on mechanical properties of coconut fibers," *IOP Conference Series: Materials Science and Engineering*, vol. 619, no. 1, article 012011, 2019.

[34] M. Arsyad and R. Soenoko, "The effects of sodium hydroxide and potassium permanganate treatment on roughness of coconut fiber surface," *MATEC Web of Conferences*, vol. 204, article 05004, 2018.

[35] C. H. Lee, A. Khalina, and S. H. Lee, "Importance of interfacial adhesion condition on characterization of plant-fiber-reinforced polymer composites: a review," *Polymers*, vol. 13, no. 3, p. 438, 2021.

[36] R. Punyamurthy, D. Sampathkumar, B. Bennehalli, R. Patel, and S. C. Venkateshappa, "Abaca fiber reinforced epoxy composites: evaluation of impact strength," *International Journal of Sciences: Basic and Applied Research (IJSBAR)*, vol. 18, no. 2, pp. 305–317, 2014.

[37] H. Hariharan and G. Rajeshkumar, "Investigation of mechanical properties of sisal fiber and sugar palm fiber reinforced hybrid composites," *Qeios*, 2024.

[38] C. Sun, J. Min, J. Lin, and H. Wan, "Effect of atmospheric pressure plasma treatment on adhesive bonding of carbon fiber reinforced polymer," *Polymers*, vol. 11, no. 1, p. 139, 2019.

[39] H. Cui and X. Gao, "Surface modification on polyimide yarn by plasma treatment to enhance adhesion with polypropylene resin," *Polymers*, vol. 14, no. 19, p. 4232, 2022.

[40] A. Chemicals, "Epoxy SL-technical data sheet. Agel Chemicals: p 3," https://agelchemicals.de/uploads/Files/pdf/EPOXY%2520SL.pdf.

[41] D. Jaiswal, G. L. Devnani, G. Rajeshkumar, M. R. Sanjay, and S. Siengchin, "Review on extraction, characterization, surface treatment and thermal degradation analysis of new cellulosic fibers as sustainable reinforcement in polymer composites," *Current Research in Green and Sustainable Chemistry*, vol. 5, p. 100271, 2022.

[42] B. Kojić-Prodić, "A century of X-ray crystallography and 2014 international year of X-ray crystallography," *Macedonian Journal of Chemistry and Chemical Engineering*, vol. 34, no. 1, pp. 19–32, 2015.

[43] M. K. Singh, R. Tewari, S. Zafar, S. M. Rangappa, and S. Siengchin, "A comprehensive review of various factors for application feasibility of natural fiber-reinforced polymer composites," *Results in Materials*, vol. 17, p. 100355, 2023.

[44] A. H. Saputra and G. Setyarso, "Vacuum infusion equipment design and the influence of reinforcement layers addition to the resin infusion time," *IOP Conference Series: Materials Science and Engineering*, vol. 162, no. 1, article 012015, 2016.

[45] M. Tolessa and B. Singh, "A review on composite materials from natural plant resources: recent trends and future potentials," *International Journal of Innovative Research in Science, Engineering and Technology*, vol. 9, no. 1, 2023.

[46] K. Bharath, M. Pasha, and B. Nizamuddin, "Characterization of natural fiber (sheep wool)-reinforced polymer-matrix composites at different operating conditions," *Journal of Industrial Textiles*, vol. 45, no. 5, pp. 730–751, 2016.

[47] P. Sahu and M. Gupta, "Water absorption behavior of cellulosic fibres polymer composites: a review on its effects and remedies," *Journal of Industrial Textiles*, vol. 51, 5 Supplement, pp. 7480S–7512S, 2022.

[48] T. R. T. Hosne Ara Begum and M. A. Shahid, "Analysis of water absorption of different natural fibers," *Journal of Textile Science and Technology*, vol. 7, no. 4, pp. 152–160, 2021.

[49] A. Patrucco, M. Zoccola, and A. Anceschi, "Exploring the potential applications of wool fibers in composite materials: A review," *Polymers*, vol. 16, no. 16, p. 2360, 2024.

[50] S. P. Subramanyam, D. K. Kotikula, B. Bennehalli et al., "Plain-woven areca sheath fiber-reinforced epoxy composites: the influence of the fiber fraction on physical and mechanical features and responses of the tribo system and machine learning modeling," *ACS Omega*, vol. 9, no. 7, pp. 8019–8036, 2024.

[51] O. Abdellaoui, T. Harizi, and S. Msahli, "Effect of the chemical unhairing process on pulled wool characteristics," *Fibres & Textiles in Eastern Europe*, vol. 30, no. 3, pp. 70–78, 2022.

[52] M. J. P. Macedo, G. S. Silva, M. C. Feitor, T. H. C. Costa, E. N. Ito, and J. D. D. Melo, "Surface modification of kapok fibers by cold plasma surface treatment," *Journal of Materials Research and Technology*, vol. 9, no. 2, pp. 2467–2476, 2020.

[53] S. Sudarisman, H. Haniel, A. K. Taufik, M. Tiopan, R. A. Himarosa, and M. A. Muflikhun, "Tensile, compressive, and flexural characterization of CFRP laminates related to water absorption," *Journal of Composites Science*, vol. 7, no. 5, p. 184, 2023.

[54] D. Rajesh, N. Lenin, R. Cep, P. Anand, and M. Elangovan, "Experimental investigation of bi-directional flax with ramie fibre-reinforced phenol-formaldehyde hybrid composites," *Polymers*, vol. 14, no. 22, p. 4887, 2022.

[55] M. H. Zin, K. Abdan, N. Mazlan, E. S. Zainudin, and K. E. Liew, "The effects of alkali treatment on the mechanical and chemical properties of pineapple leaf fibres (PALF) and adhesion to epoxy resin," *IOP Conference Series: Materials Science and Engineering*, vol. 368, no. 1, article 012035, 2018.

[56] J. Tusnim, N. S. Jenifar, and M. Hasan, "Effect of chemical treatment of jute fiber on thermo-mechanical properties of jute and sheep wool fiber reinforced hybrid polypropylene composites," *Journal of Thermoplastic Composite Materials*, vol. 35, no. 11, pp. 1981–1993, 2022.

[57] M. Bahrami, B. Enciso, C. M. Gaifami, J. Abenojar, and M. A. Martinez, "Characterization of hybrid biocomposite polybutyl-succinate/carbon fibers/flax fibers," *Composites Part B: Engineering*, vol. 221, p. 109033, 2021.

[58] S. Shahidi, A. Rashidi, M. Ghoranneviss, A. Anvari, and J. Wiener, "Plasma effects on anti-felting properties of wool fabrics," *Surface and Coatings Technology*, vol. 205, pp. S349–S354, 2010.

[59] N. Bhat and D. Upadhyay, "Plasma-induced surface modification and adhesion enhancement of polypropylene surface," *Journal of Applied Polymer Science*, vol. 86, no. 4, pp. 925–936, 2002.

[60] O. G. Agbabiaka, I. O. Oladele, and O. O. Daramola, "Mechanical and water absorption properties of alkaline treated coconut (Cocosnucifera) and sponge (Acanthus montanus) fibers reinforced polypropylene composites," *American Journal of Materials Science and Technology*, vol. 4, no. 2, pp. 84–92, 2015.

[61] N. Kumar, A. Singh, K. Debnath, and R. Ranjan, "Mechanical characterization of animal fibre-based composites," *Indian Journal of Fibre & Textile Research*, vol. 45, no. 3, pp. 293–297, 2020.

[62] D. Chakrabarti, M. S. Islam, K. Jubair, and M. R. H. Sarker, "Effect of chemical treatment on the mechanical properties of luffa fiber reinforced epoxy composite," *Journal of Engineering Advancements*, vol. 1, no. 2, pp. 37–42, 2020.

[63] F. R. Oliveira, L. Erkens, R. Fangueiro, and A. P. Souto, "Surface modification of banana fibers by DBD plasma treatment," *Plasma Chemistry and Plasma Processing*, vol. 32, no. 2, pp. 259–273, 2012.

[64] N. Sapiai, A. Jumahat, and R. N. Hakim, "Tensile and compressive properties of hybrid carbon fiber/kenaf polymer composite," *Advances in Environmental Biology*, vol. 8, no. 8, pp. 2655–2661, 2014.